

RESEARCH ACTIVITIES VII

Coordination Chemistry Laboratories

Prof. Masa-aki Haga, Prof. Takeshi Sakurai, Dr. Hideaki Monjushiro and Dr. Hidemi Nagao finished their term in March 1998 in the laboratory of Synthetic Coordination Chemistry. Prof. Haga moved to Chuou Univ. Prof. Sakurai, Dr. Monjushiro and Dr. Nagao returned to Kanazawa Univ. and Osaka Univ. Their contribution to the coordination Chemistry Laboratory (CCL) during their term is highly acknowledged. Prof. Yuzou Nishida, Prof. Yasushi Tsuji, Dr. Tomohiro Ozawa and Dr. Hiroyuki Kawaguchi took the position of Synthetic Coordination Chemistry from April 1998. Prof. Yuzou Yoshikawa (Okayama Univ.) and Assoc. Prof. Hiroshi Nakazawa (Hiroshima Univ.) finished their term as Adjunct Prof. in March 1998 in the Laboratory of Coordination Bond. Their effort during their term is gratefully appreciated. Prof. Ginya Adachi (Osaka Univ.) and Assoc. Prof. Hiromi Tobita (Tohoku Univ.) continued their position as Adjunct Prof. of Laboratory of Coordination Bond. Prof. Hiromu Sakurai (Kyoto Pharmacy Univ.) and Assoc. Prof. Yuji Mizobe (Univ. Tokyo) took the position of the laboratory of Complex Catalysis.

VII-A Surface Coordination Chemistry towards Molecular Protonic Devices

The design and fabrication of molecular arrays or layers at the surface is one of the important and attractive area in the future material science. In order to control the molecular arrays in two dimensions, the incorporation with coordination bond has advantage compared to the other molecular interactions such as hydrogen bonding and electrostatic interaction from the viewpoint of strength of interaction and molecular geometry around metal ion. However, the incorporation with coordination bond at the interface has not extensively studied so far. Our aim is to construct a supramolecular assembly in the controlled manner through the coordination bond at the surface, and to search an electrochemical and photochemical function towards the molecular electronic devices. We have developed the chemical principle underlying the proton-induced switching in 2-(2-pyridyl)benzimidazole Ru complexes. In order to achieve the proton-induced switching systems, the interlocking between the potential change by protonation/deprotonation and the pKa change by Ru(II) to Ru(III) oxidation is responsible. The judicious molecular design of the Ru complexes containing benzimidazole ligands allows us to synthesize the novel supramolecular metal complexes with bistable property not only in solution but also at the surface. Our synthetic strategy is the following: (1) The intrinsic properties of molecular inorganic complex are thoroughly examined from the viewpoint of photoactive, electroactive, or proton-responsive building blocks for molecular devices. (2) The molecular inorganic complex modules are organized or integrated for building up the molecular assemblies. Particularly, "complexes-as-ligands" method is useful to synthesize the supramolecular systems.

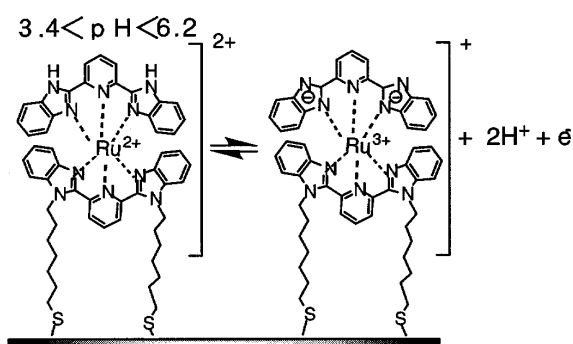
VII-A-1 Proton-Coupled Electron Transfer Reaction of Self-Assembled Monolayer of Ruthenium(II) Complex Containing Tridentate 2,6-Bis(benzimidazol-2-yl)pyridine

Masa-aki HAGA, Hun-Gi HONG, Hideaki MONJUSHIRO, Yasushi KAWATA and Ryuichi ARAKAWA

[Langmuir submitted]

The self assembled monolayer(SAM) of novel bis-[Ru(bzimpyH₂)(bzimpy)]-substituted octyl disulfide(1) and mixed monolayers with octanethiol on a polycrystalline gold electrode were characterized by means of MALDI-TOF mass spectrometry, XPS, and cyclic voltammetry. The shape of cyclic voltammograms for Ru(II/III) couple is strongly dependent on the surface coverage, and is close to the ideal voltammogram for the monolayer species. The oxidation potential of the Ru monolayer shows a linear dependence on solution pH, which indicates that the proton-coupled oxidative reactions occurred on the gold surface. The pKa values of Ru(bzimpyH₂) group on the gold surface were determined from the analysis for the plot of the oxidation potential vs pH. The pKa values of SAM

depend on the amounts of surface coverage because of the change of localized pH.



Scheme 1. Proton-coupled Redox Reaction of Ru Complex (1).

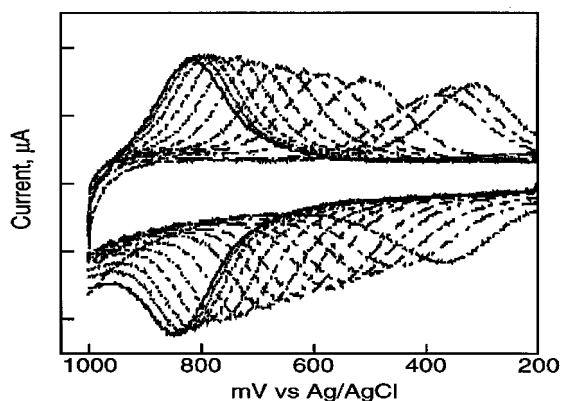


Figure 1. pH Dependence of cyclic voltammograms of the Ru complex modified on Au (From right to left, pH 1.33, 1.83, 2.21, 2.59, 3.10, 3.58, 4.09, 4.52, 4.86, 5.36, 5.83, 6.35, 6.88, and 7.35 respectively)

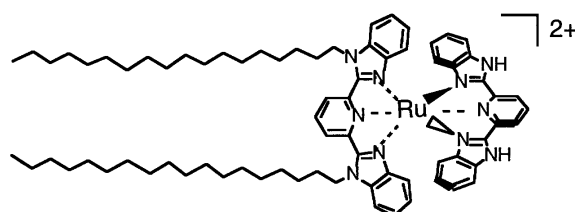
VII-A-2 Proton-Coupled Electron Transfer Reaction of Langmuir-Blodgett Monolayer of Ruthenium(II) Complex Containing Tridentate 2,6-Bis(benzimidazol-2-yl)pyridine

Masa-aki HAGA, Hun-Gi HONG, Hideaki MONJUSHIRO and Kezhi WANG

Proton translocation coupled to redox reaction is often seen in a biological membrane, and plays an important role for the energy transduction. In the present paper, we report the electrochemical pH response of Ru(II) complex Langmuir-Blodgett films on an indium-tin oxide (ITO) glass in order to simulate such a direction-controlled proton translocation. A novel amphiphilic Ru complex containing 2,6-bis(benzimidazolyl)pyridine group in Scheme 1, $[\text{Ru}(\text{L18})(\text{bimpyH}_2)]^{2+}$ (**1**) (L18 = 2,6-bis(2'-(1'-octadecylbenzimidazolyl)pyridine); bimpyH₂ = 2,6-bis(2'-benzimidazolyl)pyridine), was synthesized. This Ru complex **1** acts as a diprotic acid ($\text{pK}_{\text{a}1} \sim 5.35$ and $\text{pK}_{\text{a}2} \sim 6.94$ in Triton micelle condition). Surface pressure-area (-A) isotherms of this complex **1** are strongly dependent on the subphase pH (Figure 1). At the subphase pH = 2.89, a phase transition was observed at surface pressure at 20 mNm^{-1} . The molecular area obtained from the second condensed solid state is 1.3 nm^2 molecules⁻¹, which is almost coincided with that obtained at the subphase pH = 9.21. Proton equilibria at the air-water interface were also observed by *in situ* UV spectra. The vertical molecular orientation at the air-water interface was also proved from *in situ* UV spectra by the selection rule of metal-to-ligand charge transfer (MLCT) band around 500 nm. The Ru complex **1** was successfully transferred from the subphase onto the ITO glass with the transfer ratio of nearly 1 both at pH 2.89 and 9.21. The absorption maxima of MLCT band around 500 nm in the transferred LB films is shifted to a longer wavelength, accompanied by changing the subphase pH from 2.89 to 9.21. This trend is exactly consistent with the solution chemistry. The plot of absorbance vs the number of layers gave a linear line, which indicates a good measure of multilayer formation.

Cyclic voltammograms of Ru complex monolayer

on an ITO electrode at different pH are shown in Figure 2. At pH 1.7, the peak-to-peak separation for the film transferred at 25 mNm^{-1} was 42 mV and the peak width at half-height was 140 mV. The transferred surface pressure affects the peak width at half-height: *i.e.*, lower pressure gave smaller peak width. Among the pH region of $1 < \text{pH} < 8$, the oxidation potential is linearly shifted to a negative direction when the solution pH is increased. This indicates proton-coupled redox reaction occurred.



Scheme 1. Structure of $[\text{Ru}(\text{L18})(\text{bimpyH}_2)]^{2+}$ (**1**)

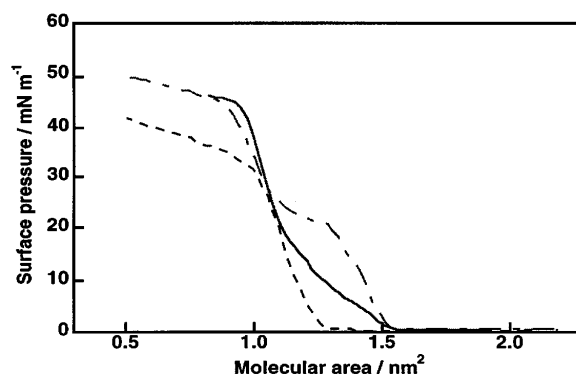


Figure 1. -A isotherm of Ru complex **1** at different pH subphases at 20°C. (pH 2.89 (---), 5.40 (—) and 9.21 (- - -))

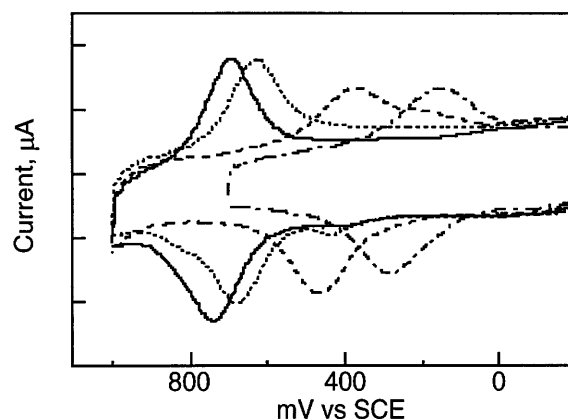


Figure 2. Cyclic voltammograms of Ru complex LB monolayer films on ITO in different pH: pH = 1.59, 2.66, 5.55 and 9.61 from left to right.

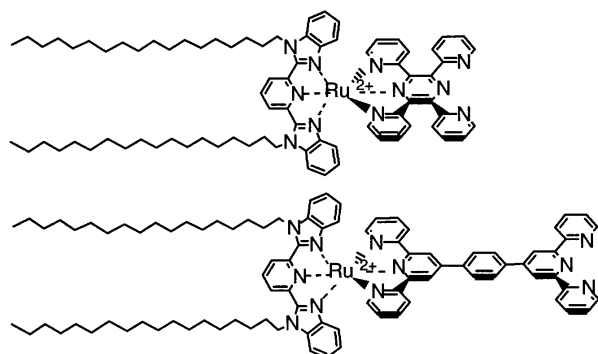
VII-A-3 Metal Coordination to Amphiphilic Ru Complexes at the Air-Water Interface

Masa-aki HAGA, Noriaki KATO, Hideaki MONJUSHIRO and Kezhi WANG

[*J. Supramol. Sci.* in press]

We have examined the applicability of "metal

complex as a ligand" strategy at the interface by using the Ru complexes acting as a ligand. New amphiphilic ruthenium complexes containing 2,6-bis(N-octadecylbenzimidazolyl)-pyridine (L18), $[\text{Ru}(\text{L18})(\text{X})]^{2+}$, were synthesized, where $\text{X} = 2,3,5,6$ -tetrakis(2'-pyridyl)pyrazine (tppz) and 1,4-bis(2,2':6', 2''-terpyridine-4'-yl)benzene (bteb), in which the bis-tridentate ligand (tppz or bteb) of $[\text{Ru}(\text{L18})(\text{X})]^{2+}$ can act not only as a hydrophilic head group but also as a coordination site to a metal ion from the subphase at the air-water interface. These amphiphilic Ru complexes lead to a stable Langmuir-Blodgett (LB) film formation. The incorporation of metal ion from subphase at the air-water interface was proved by the measurements of π -A isotherms, UV spectra, angular dependent XPS spectra. The AFM images showed the formation of a circular domain structure at low surface pressures. The domains gathered with progressive compression. The weak intermolecular interaction between the Ru complexes is responsible for the domain formation at the air-water interface.



Scheme 1. Structure of amphiphilic Ru complex

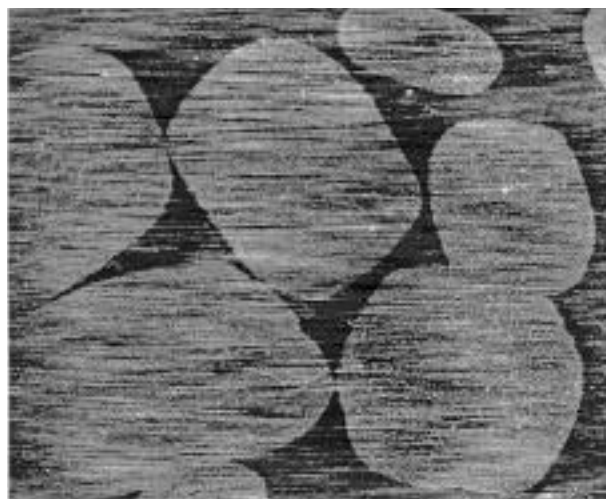


Figure 1. AFM image ($5 \mu\text{m} \times 5 \mu\text{m}$) of the LB monolayer film of $[\text{Ru}(\text{L18})(\text{tppz})](\text{PF}_6)_2$ transferred onto mica at a surface pressure of 10 mNm^{-1} .

VII-A-4 Synthesis and Characterization of Amphiphilic Ru Complex with 2,2':6',2''-Terpyridine-4'-phosphonic Acid at the Air-Water Interface

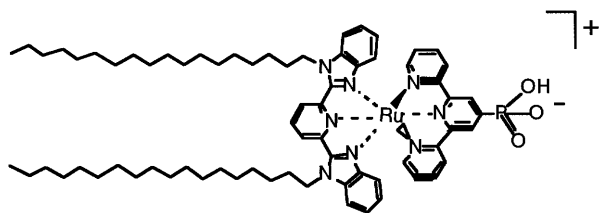
Kezhi WANG, Md. Delower HOSSAIN, and Hideaki MONJUSHIRO and Masa-aki HAGA

[Langmuir submitted]

A novel amphiphilic Ru(II) complex with its molecular structure shown below, $\text{Ru}(\text{L18})(\text{tpy-PO}_3\text{H})\text{-PF}_6$ ($\text{L18} = 2,6$ -bis(N-octadecylbenzimidazolyl)pyridine and $\text{tpy-PO}_3\text{H} =$ monoprotonated-2,2':6'',2''-terpyridine-4-phosphonate), was designed and synthesized for this purpose.

Surface pressure-area (π -A) isotherms were measured in detail by changing a subphase condition such as pH or metal ion (Zn^{2+} , Cd^{2+} and Mn^{2+}). A freshly prepared dichloroethane solution of the complex (1.8 - 2.5 mg/5ml) was spread on the various subphases. The complex had a stable Langmuir-film forming property with a limiting molecular area of $1.4 \text{ nm}^2 \cdot \text{molecule}^{-1}$, which is consistent with that observed previously for $[\text{Ru}(\text{L18})(\text{tppz})]^{2+}$ ($\text{tppz} = 2,3,5,6$ -tertakis(2'-pyridyl)pyrazine). The π -A isotherms are strongly dependent on the subphase pH. An expansion of the limiting molecular area was observed with increasing the subphase pH. In *in-situ* uv-vis spectra, we found that the Ru-to-ligand charge transfer (MLCT) band at the air-water interface is very sensitive to the subphase conditions, which is relevant to the molecular orientation of Ru complex. The intensity of MLCT band at the air-water interface was suppressed at pH 2.8 compared to that for the solution spectra, but at pH 9.4 the normal MLCT intensity was obtained. Thus, the molecular orientation of Ru complex can be controlled by the solution pH. Transferred LB films on hydrophilic and hydrophobic glass substrates have been studied by uv-vis, angle-resolved X-ray photoelectron spectroscopy (XPS), low angle x-ray diffraction (XRD), cyclic voltammetry and atomic force microscopy. A plot of absorbance at $\lambda = 340 \text{ nm}$ of LB films prepared at various experimental conditions used, as a function of number of LB layers is a straight line, indicative of a reproducible film transfer. Further, the transfer ratio onto an ITO substrate falls within $0.9 \sim 1$.

When the metal ion contained subphase was used, the monolayer became stabilized as expected. Molar ratios of the Ru complex to the metal ions (Zn^{2+} , Cd^{2+} and Mn^{2+}) in the transferred LB films from the corresponding metal ion-containing subphases, were found to be approximately 1:1, consistent with known layered solid of divalent metal organophosphonates, $\text{M}(\text{O}_3\text{PR})\text{H}_2\text{O}$ ($\text{M} = \text{Mg}, \text{Mn}, \text{Zn}, \text{Cd}$; $\text{R} = \text{n-alkyl}, \text{aryl}$ groups). A similar structure could thus be inferred for our case. Furthermore, an angle-resolved XPS of transferred LB films from metal ion contained subphase revealed that the relative intensity ratio of Ru $3d_{5/2}$ to metal ion peak reveals the angular dependence due to ordered layered structure of the LB films. Cyclic voltammetry of the monolayer film on ITO working electrode in 0.1 M HClO_4 as supporting electrolyte showed a reversible oxidation wave at $+1.02 \text{ V}$ vs SCE which is independent of pH. Furthermore, $[\text{Ru}(\text{L18})(\text{tpy-PO}_3\text{H})]\text{-TiO}_2$ composite was successfully transferred onto an ITO electrode when the exfoliated TiO_2 suspension was used as a subphase, which shows a photoelectrochemical response.



Scheme 1. The structure of Ru complex, Ru(L18)(tpy-PO₃H)PF₆

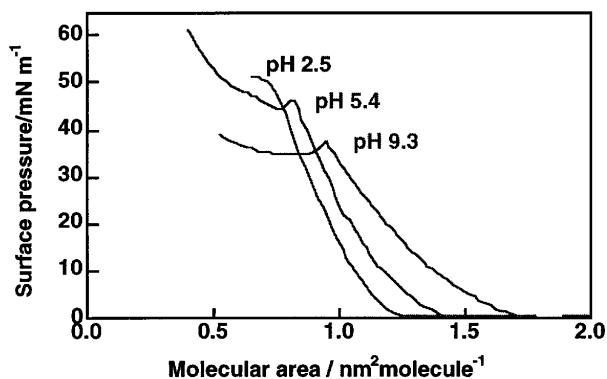


Figure 1. pH Dependence of subphase on -A isotherms for Ru(L18)(tpy-PO₃H)PF₆ at 20°C.

VII-A-5 Metal-to-Ligand Charge Transfer (MLCT) Band of [Ru(L18)(tridentate ligand)]²⁺ as a Molecular Orientation Probe at the Air-water Interface

Masa-aki HAGA, Kezhi WANG, Yuzo NISHIDA and Hideaki MONJUSHIRO (*Osaka Univ.*)

[submitted]

Metal-to-ligand charge transfer (MLCT) band of Ru(II) complexes has been investigated in detail for the last few decades. The present Ru(II) complexes, [Ru(L18)(tridentate ligand)]²⁺, where L18 = 2,6-bis(N-octadecylbenzimidazolyl)pyridine and tridentate ligand = 2,3,5,6-tertakis(2'-pyridyl)pyrazine etc, which has a C₂ symmetry, show a characteristic MLCT band around 500 nm. Considering the molecular symmetry of these Ru complexes, the MLCT transition is polarized to z axis. Therefore, the drastic change of absorption intensity on MLCT band is expected when all the molecules of Ru complex is oriented to the z-axis direction. The *in-situ* UV spectra of [Ru(L18)(tppz)]²⁺ shows a drastic decrease of MLCT band around 500 nm, which indicates the vertical orientation of molecules with respect to the air-water interface. On the other hand, a clear MLCT band of [Ru(L18)(betb)]²⁺ (betb = 1,4-bis(2,2':6',2''-terpyridine-4'-yl)benzene) was

observed around 500 nm at the air-water interface. When the addition of Cu²⁺ ion into the subphase for [Ru(L18)(betb)]²⁺, the MLCT band was disappeared but the π - π^* bands are still observed. (Figure 1) This spectral change was rationalized by the change of molecular orientation from tilted form to vertical one by the Cu²⁺ ion coordination from the subphase. This interpretation was further supported by the surface pressure-area isotherm measurement. Therefore, the MLCT band of [Ru(L18)(tridentate ligand)]²⁺ acts as a molecular orientation probe at the air-water interface.

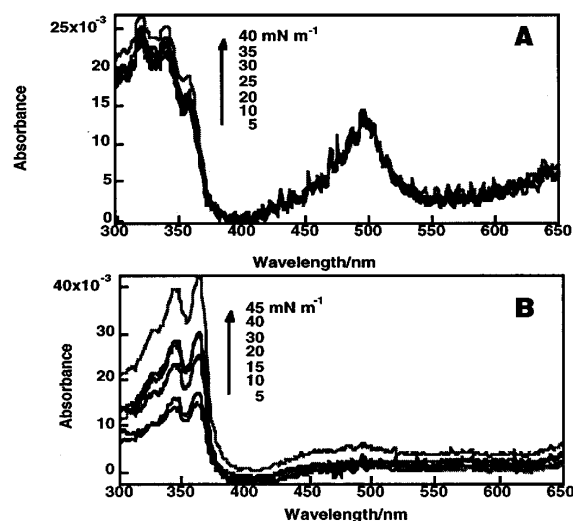
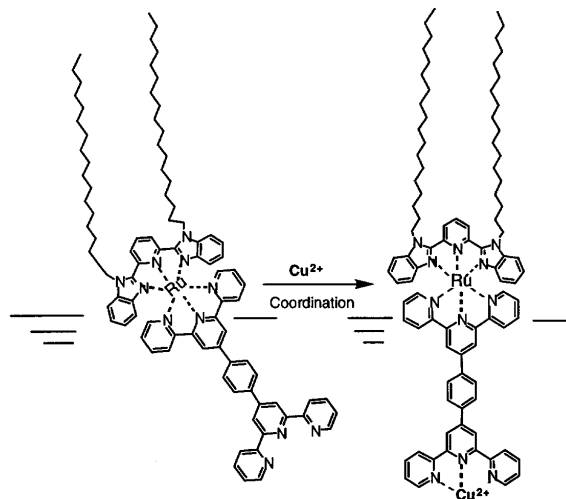


Figure 1. *in-situ* UV spectra of [Ru(L18)(betb)]²⁺ by Cu²⁺ coordination: (A) On a pure water subphase (B) on a Cu²⁺ (1 mM) containing subphase.



Scheme 1. The change of molecular orientation from tilted form to vertical one by the Cu²⁺ ion coordination from the subphase

VII-B Redox Chemistry of Inorganic Metal Complexes

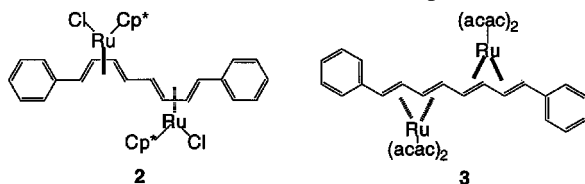
The fundamental understanding and deeper knowledge of the redox processes in inorganic metal complexes are needed in order to build in the supramolecular inorganic complexes as components of molecular based devices. Molecular electrochemistry of inorganic and organometallic metal complexes in solution has been investigated in order to elucidate the redox chemistry of metal complexes and get relationships between structure and electrochemical behavior.

VII-B-1 1,8-Diphenyl-octa-1,3,5,7-tetraene Complexes of Ruthenium(II): Crystal Structures of $[\mu\text{-}(s\text{-}cis\text{-}1,2,3,4\text{-} : s\text{-}cis\text{-}5,6,7,8\text{-} -\text{PhCH}=\text{CHCH}=\text{CHCH}=\text{CHCH}=\text{CHPh})(\text{RuClCp}^*)_2]$ and $[\mu\text{-}(s\text{-}trans\text{-}1,2,3,4\text{-} : s\text{-}trans\text{-}5,6,7,8\text{-} -\text{PhCH}=\text{CHCH}=\text{CHCH}=\text{CHCH}=\text{CHPh})\text{-}\{\text{Ru}(\text{acac})_2\}_2]$

Kazushi MASHIMA (*Osaka Univ*), **Hiroki FUKUMOTO** (*Osaka Univ*), **Kazuhide TANI** (*Osaka Univ*), **Masa-aki HAGA** and **Akira NAKAMURA** (*Osaka Univ*)

[*Organometallics* 17, 410 (1998)]

Reaction of 1,8-diphenyl-1,3,5,7-octatetraene with $[\text{Ru}(\mu\text{-Cl})\text{Cp}^*]_4$ (**1**) ($\text{Cp}^* = 5\text{-pentamethylcyclopentadienyl}$) gave $[\mu\text{-}(s\text{-}cis\text{-}1,2,3,4\text{-} : s\text{-}cis\text{-}5,6,7,8\text{-} -\text{PhCH}=\text{CHCH}=\text{CHCH}=\text{CHCH}=\text{CHPh})(\text{RuClCp}^*)_2]$ (**2**), whose crystal structure revealed that **2** has a planar tetraene backbone coordinated by two Cp^*RuCl moieties in *s-cis*-⁴-fashion; while the reaction with $\text{Ru}(\text{acac})_3/\text{Zn}$ system resulted in the formation of $[\mu\text{-}(s\text{-}trans\text{-}1,2,3,4\text{-} : s\text{-}trans\text{-}5,6,7,8\text{-} -\text{PhCH}=\text{CHCH}=\text{CHCH}=\text{CHCH}=\text{CHPh})\{\text{Ru}(\text{acac})_2\}_2]$ (**3**), where both of the two $\text{Ru}(\text{acac})_2$ moieties prefer *s-trans* coordination and thus the plane of the octatetraene backbone of **3** is deformed into an S-shape. Electrochemical studies for complexes **2** and **3** revealed that complex **3** has a strong coupling between the two ruthenium centers and is a conjugatively interacted d-p organometallic system, whereas complex **2** has a longer -conjugation of the tetraene backbone without electronic communication between the two RuClCp^* moieties



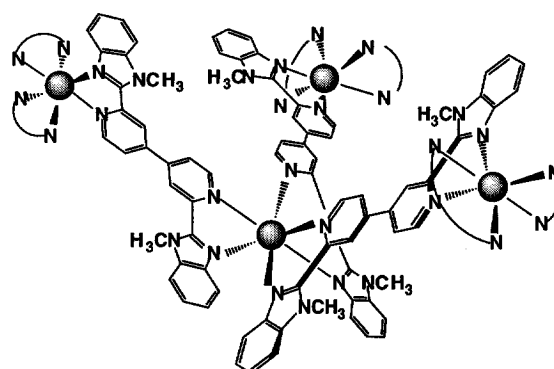
VII-B-2 Spectroelectrochemical Analysis of Intervalence Band in Mixed-Valence Di- and Tetranuclear Ru Complexes by Flow-Through Method

Masa-aki HAGA, **Md. Meser ALI** (*Mie Univ*), **Hiroyasu SATO** (*Mie Univ*), **Hideaki MONJUSHIRO**, **Koichi NOZAKI** (*Osaka Univ*) and **Kenji KANO** (*Kyoto Univ*)

[*Inorg. Chem.* 37, 2320 (1998)]

Novel dendritic tetranuclear Ru and Os-2,2'-bipyridine complexes bridged by 2,2'-bis(1-methylbenzimidazo-2-yl)-4,4'-bipyridine (Scheme 1) showed four closely spaced one-electron oxidation processes; i.e., the central one-electron oxidation occurs first,

followed by three peripheral metal oxidations at almost same potentials. During the progress of electrochemical oxidation, a characteristic near-infrared(NIR) band was observed, which can be assigned to intervalence charge transfer (IT) transition within the mixed-valence state. Since the potential separations among these three processes are generally small, the selective oxidation could not be achieved and even the one-electron oxidized species might be easily disproportionated into the original and two electron oxidized species. Therefore, the accurate determination of the absorption spectra for the mixed valence complexes should be determined by considering the comproportionation equilibria. In order to reconstruct the corrected absorption spectra of each mixed-valence complex, we have developed a new spectral analysis method based on the combination of digital simulation analysis of the reversible CV curves and the electrochemical titration by flow-through cell (Figure 2), which gives the complete spectra of IT band for the partially oxidized species in the dendritic tetranuclear complexes. This method can be applicable not only for the dendritic Ru tetranuclear complexes but also dinuclear Ru complexes.



Scheme 1. Structure of dendritic tetranuclear Ru/Os-2,2'-bipyridine complexes

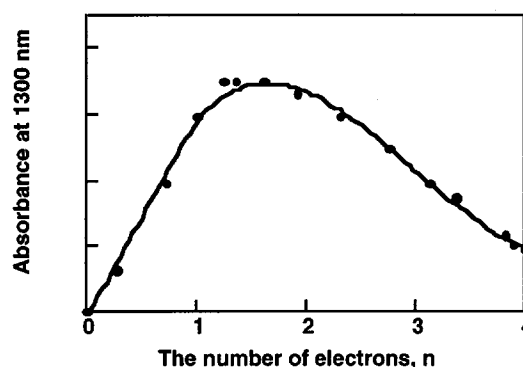


Figure 1. A plot of absorbance at 1300 nm vs the number of electrons, n , obtained from the current ratio for the complex, $[\{(\text{bpy})_2\text{Ru}(\text{dmbbbpy})\}_3\text{Ru}]^{8+}$ (2.3×10^{-4} M)

VII-C New Insight into Mechanism of Biological Oxygenation Reactions

One of the remaining frontiers in organic chemistry is the direct functionalization of saturated hydrocarbons. The catalytic cycle that oxidizes a hydrocarbon RH to an alcohol R-OH employing cytochrome P-450 and methane monooxygenase is a well-established reaction, however, no reasonable mechanism for activation of dioxygen and for formation of a R-OH is available at present. Recently the present author has proposed a new idea that elucidates many biological oxygenation reactions comprehensively. In this consideration, the importance of electrophilic nature of a metal-peroxide adduct and role of the substrate as an electron donor were emphasized. This idea suggests that formation of a high-valent iron-oxo species occurs most likely when the metal-peroxide intermediate is activated through electronic interaction with both the peripheral organic group and substrate; the latter two act as an electron donor to the peroxide adduct. We are now continuing the study on the reactivity of the metal-peroxide adduct in order to ascertain that my idea is applicable to other reactions, such as degradation of DNA and proteins, etc.

VII-C-1 Mechanism of Double-Strand DNA Cleavage Effected by Iron-Bleomycin

Teruyuki KOBAYASHI, Li Li GUO and Yuzo NISHIDA

[*Z. Naturforsch.* **53C** (1998) in press]

We have observed that in the absence of hydrogen peroxide the Fe(III)-bleomycin (BLM) complex exhibits high DNA cleavage efficiency converting supercoiled Form I DNA (pBR322 or λ 174) to Form II (nicked, relaxed circular); the present study may give an important clue to elucidate the fact that iron-bleomycin mediated double-strand DNA cleavage requires at least one molecule of oxygen(O₂) over the amount required to form "activated bleomycin."

VII-C-2 Contribution of a Peroxide Adduct of Copper(II)-Peptide Complex to Modify the Secondary Structure of Albumin

Yoshihiro ISHIKAWA, Sayo ITO, Satoshi NISHINO, Shigeru OHBA and Yuzo NISHIDA

[*Z. Naturforsch.* **53C**, 378 (1998)]

We have found that copper(II) compounds containing a peptide group in the chelate exhibit high activity for modification or degradation of albumin in the presence of hydrogen peroxide, whereas no activity was detected for the copper(II) complexes without an amide-group. It is suggested that presence of amide group in the ligand may play an important role in the formation of the peroxide adduct and in activation of the peroxide ion, leading to cleavage of peptide bond of a neighboring protein. It is implied that conversion of normal cellular prion protein PrP^C into a disease-causing isoform, PrP^{Sc} is attributed to the activated peroxide ion coordinated to a copper(II) ion captured in the NH₂-terminal domain of PrP^C.

VII-D Metal Ions in Biological Systems

In order to reveal the biological roles of transition metal ions, structures and reactions of metalloproteins and metalloenzymes such as NO reductase, laccase, ascorbate oxidase, and several blue copper proteins have been studied by absorption, CD, MCD, and EPR spectroscopies and by magnetic susceptibility measurements. V-haloperoxidase has also been isolated and characterized.

VII-D-1 Isolation and Characterization of Nitric Oxide Reductase from *Paracoccus halodenitrificans*

Nobuhiko SAKURAI and Takeshi SAKURAI

[*Biochemistry* **36**, 13809 (1997)]

Nitric oxide reductase was isolated from the membrane fraction of a denitrifying bacterium, *Paracoccus halodenitrificans*, in the presence of n-dodecyl- β -D-maltoside. A relatively simple and effective procedure to purify NO reductase using DEAE-Toyoppearl and hydroxyapatite (ceramic) chromatographies has been developed. The enzyme consisted of two subunits with molecular masses of 20 and 42 kDa associated with the *c* type heme and two *b*

type hemes, respectively. The optical and MCD spectra of the oxidized (as isolated) and reduced enzymes indicated that the heme *c* is in the low spin state and the hemes *b* are in the high and low spin states. The EPR spectrum also showed the presence of the split high spin component ($g = 6.6, 6.0$) and two low spin components ($g_z, y, x = 2.96, 2.26, 1.46, g_z = 3.59$). Although the presence of an extra iron was suggested from atomic absorption spectroscopy, a non-heme iron could not be detected by colorimetric titrations using ferene and nitro-PAPS. One of extra signals at $g = 4.3$ and 2.00 might come from a non-heme iron, while they may originate from an adventitious iron and a certain non-metallic radical, respectively. When CO acted on the reduced enzyme, both of the low spin hemes were not affected, and when NO acted on the reduced enzyme, the optical and MCD spectra were of a mixture of the

oxidized and reduced enzymes. Consequently, the reduction of NO was supposed to take place at the high spin heme *b*. The heme *c* and the low spin heme *b* centers were considered to function as electron mediators during the intermolecular and intramolecular processes.

VII-D-2 Spectral Properties of Cytochrome *c*₅₅₃ and a Membrane-Bound Cytochrome *b* from *Alcaligenes xylooxidans* GIFU 1051

Nobuhiko SAKURAI, Hideyuki KUMITA (*Nagoya Inst. Tech.*), Takeshi SAKURAI and Hideki MASUDA (*Nagoya Inst. Tech.*)

[*Bull. Chem. Soc. Jpn.* **70**, 135 (1998)]

Cytochrome *c*₅₅₃ and cytochrome *b* were isolated from soluble and membrane fractions of *Alcaligenes xylooxidans* GIFU 1051, respectively, and their spectroscopic characterization has been performed. Cytochrome *c*₅₅₃ has been shown to be in the low spin state both in the oxidized and reduced forms at room temperature by the absorption and magnetic circular dichroism (MCD) spectra, while the high spin heme has been also observed in the cryogenic electron paramagnetic resonance (EPR) spectra. Exogenous small ligands such as NO and CO bind to cytochrome *c*₅₅₃ by expelling the axial His ligand. The membrane-bound cytochrome *b* has two heme *b* centers in a protein molecule which are the active centers of NO reductase, the cytochrome *bc* complex, although the enzyme activity was considerably low. The absorption, MCD, and EPR spectra of the membrane-bound cytochrome *b* showed that two heme *b* centers are in the different electronic states, the high and low spin states. Cytochrome *c*₅₅₃ is the natural electron donor to the membrane-bound NO reductase, although the interprotein electron-transfer could not be studied because of the low enzyme activity of the cytochrome *b* subunit

VII-D-3 Observation of Cu-N₃⁻ Stretching and N₃⁻ Asymmetric Stretching Bands for Mono-Azide Adduct of *Rhus vernicifera* Laccase

Shun HIROTA (*Nagoya Univ.*), Hiroki MATSUMOTO (*Nagoya Univ.*), Hong-wei HUANG, Takeshi SAKURAI, Teizo KITAGAWA and Osamu YAMAUCHI (*Nagoya Univ.*)

[*Biochem. Biophys. Res. Commun.* **243**, 435 (1998)]

Mono-azide adduct of *Rhus vernicifera* laccase was investigated with resonance Raman and FT-IR spectroscopies as a step forward elucidation of the structure and function of the trinuclear center. The Cu-N₃⁻ stretching RR band was observed for azide-bound multicopper oxidases for the first time. The Cu-N₃⁻ band was located at 400 cm⁻¹ for mono-¹⁴N₃⁻ laccase, which shifted to 396 cm⁻¹ with the ¹⁵N¹⁴N¹⁴N⁻ analog. The Cu-N₃⁻ asymmetric stretching band was observed by FT-IR spectroscopy at 2035 cm⁻¹ for ¹⁴N₃⁻ laccase and at 2025 cm⁻¹ with the ¹⁵N¹⁴N¹⁴N⁻ analog. These

spectra were comparable with those for hemocyanin with a stronger π back donation from the copper to the bound N₃⁻ molecule.

VII-D-4 Genomic Cloning of the Region Encoding Nitric Oxide Reductase in *Paracoccus halodenitrificans* and a Structure Model Relevant to Cytochrome Oxidase

Nobuhiko SAKURAI and Takeshi SAKURAI

[*Biochem. Biophys. Res. Commun.* **243**, 400 (1998)]

The structural genes for the NO reductase in *Paracoccus halodenitrificans*, *norC*, *norB*, and *norQ* were sequenced. The *norC* and *norB* encode the cytochrome *c* (NorC) and cytochrome *b* (NorB) subunits, respectively. The matured NorC (17258 Da, 148 residues) has a binding motif (CXYCH) for heme *c*, which is axially coordinated by His65 and Met115. NorB (52337 Da, 451 residues) has twelve putative transmembrane helices and the 19% sequence homology with the subunit I of cytochrome oxidase from *Paracoccus denitrificans*. Several histidine and glutamate residues were identified as the ligands for two hemes *b* and *a* non-heme iron in comparison with the sequence of cytochrome oxidase. The higher-order model structures constructed from the amino acid sequences of NorC and NorB showed the topology of the helical segments and the locations of the metal centers.

VII-D-5 Magnetic Studies of the Trinuclear Center in Laccase and Ascorbate Oxidase Approached by EPR Spectroscopy and Magnetic Susceptibility Measurements

Hong-wei HUANG, Takeshi SAKURAI, Hideaki MONJUSHIRO and Sadamu TAKEDA

[*Biochim. Biophys. Acta* **160**, 1384 (1998)]

The trinuclear centers in laccase and ascorbate oxidase have been studied by EPR spectroscopy and magnetic susceptibility measurements over the wide range of temperature, 5 K to 300 K. The EPR spectra showed that type 2 Cu receives increasing tetrahedral distortion with raising temperature. Magnetic susceptibilities of laccase showed that both of type 1 and type 2 Cu's are almost fully paramagnetic since the antiferromagnetic interaction between type 3 Cu's is extremely strong from 5 K to 300 K. On the other hand, the effective magnetic moment of ascorbate oxidase is contributed by ca. 1.7 Cu²⁺ even below ca. 100 K, since type 2 Cu is partly in the reduced form. The effective magnetic moment continuously increased with raising temperature because the antiferromagnetic interaction between type 3 Cu's is not as strong as in the case of laccase. The type 2 Cu EPR signals in laccase and ascorbate oxidase were conspicuously broadened with raising temperature because of the increasing contribution of the triplet state by type 3 Cu's and/or of the rapid relaxation which finally led to only ca. 30 % detection of the type 2 Cu signal at room temperature.

The stepwise binding of azide to one of type 3 Cu's made the type 3 Cu to be EPR detectable. According to the SQUID measurements type 2 Cu and one of type 3 Cu's antiferromagnetically coupled through a bridging group, possibly not an azide ion but a hydroxide ion. All these findings indicate that the steric structure and magnetic property of the trinuclear center change depending on temperature and the magnetic data at room temperature reflect the inherent property of the trinuclear center composed of type 2 and type 3 Cu's in multicopper oxidases.

VII-D-6 Isolation and Characterization of Vanadium Bromoperoxidase from a Marine Macroalga, *Ecklonia stolonifera*

Isao HARA and Takeshi SAKURAI

[*J. Inorg. Biochem.* in press]

The bromoperoxidase has been isolated from the brown seaweed *Ecklonia stolonifera* (83 kDa) and has been characterized. Bromoperoxidase requires vanadium for enzyme activity as has been evidenced by EPR spectroscopy. On addition of V^{5+} to the isolated enzyme, the enzyme activity was increased ca. 250%, indicating that more than 2/3 of the protein molecules were in the apo form. The increases in the enzyme activity was specific to V^{5+} , while Fe^{2+} , Fe^{3+} , and Cu^{2+} inhibited the enzyme activity. This V^{5+} addition effect was inhibited in the phosphate buffer, probably because phosphate and vanadate compete for the active site. The present bromoperoxidase exhibited a high thermostability ($T_m = 68^\circ C$) and a high stability in organic solvents (completely intact even in the presence of 50 % of methanol, ethanol and 1-propanol).

VII-D-7 EPR and Magnetic Susceptibility Studies of the Trinuclear Copper Center in Native and Azide-Reacted Zucchini Ascorbate Oxidase

Hong-wei HUANG, Takeshi SAKURAI, Silvana MARITANO (*Osaka Univ.*), Augusto MARCHESINI (*Ist. Sper. per la Nut. delle Piante*) and Shinnichiro SUZUKI (*Osaka Univ.*)

[*J. Inorg. Biol. Chem.* submitted]

The magnetic properties of the trinuclear center composed of type 2 Cu and a pair of type 3 Cu's in zucchini ascorbate oxidase have been studied by EPR spectroscopy and magnetic susceptibility measurements from cryogenic temperature to room temperature. The temperature-dependent EPR spectra showed that the Az value of the type 2 Cu signal decreases with increasing temperature. Concomitantly, the type 2 Cu signal was appreciably broadened at > 150 K differing from the type 1 Cu signal. While the EPR spectrum can be simulated for the 1 : 0.3-0.4 ratio of type 1 Cu and type 2 Cu per protein molecule, the total amount of the EPR detectable Cu^{2+} was not 1.3-1.4 but was 1.7-1.8 at < 150 K and 1.3-1.4 at room temperature (Ascorbate oxidase is homodimer in which each subunit contains 1

type 1 Cu, 1 type 2 Cu and a pair of type 3 Cu's). The effective magnetic moment determined by SQUID measurements was 2.4 B. M. at < 200 K, the value for 1.7 free spins per protein molecule. However, the magnetic moment increased at > 200 K, reaching 3.2 B. M. at room temperature, the value for 2.3 free spins. This decrease in the EPR detectable amount of Cu^{2+} and the increase in magnetic moment with increasing temperature are due to the contribution of the triplet state by the antiferromagnetically coupled type 3 Cu's. The two-step binding of azide to the trinuclear center perturbs magnetic properties of the trinuclear center. Although no bridging group exists in the trinuclear center of the azide-ascorbate oxidase according to the X-ray crystal structure (Messerschmidt et al., *J. Mol. Biol.* **230**, 997-1014 (1993)), the magnetic susceptibility data indicated that two coppers in the trinuclear center are antiferromagnetically coupled. The binding modes for the one- and two-azide bound forms were discussed based on the temperature-dependent EPR and magnetic susceptibility data.

VII-D-8 The Putative Proton-Transfer Pathway in Membrane-Bound Nitric Oxide Reductase in Connection with Proton Transfers in Heme-Cu Terminal Oxidases

Takeshi SAKURAI and Nobuhiko SAKURAI

[*FEBS Lett.* submitted]

The amino acid sequence of the membrane-bound nitric oxide reductase from *Paracoccus halodenitrificans* was compared with that of cytochrome oxidase. There were strong similarities between NO reductase and cytochrome oxidase for the presence and topology of the twelve-transmembrane segments and the ligand groups for metal centers. In addition, it was also found that the acidic amino acids to assist the transfer of the vectorial proton from cytoplasm to the Heme a_3 -CuB center in cytochrome oxidase are also present in the cytochrome *b* subunit of NO reductase, although the amino acids to transfer the vectorial proton from Heme a_3 -CuB to periplasm and those to transfer the scalar proton are absent in NO reductase. This suggests the possibility of the presence of a specific pathway to transport protons utilized to transform 2NO to N_2O and H_2O at the binuclear center composed of the high spin heme *b* and the non-heme iron. This pathway to transport protons to be reacted might have evolved into the vectorial proton transfer pathway in cytochrome oxidase.

VII-D-9 Roles of Four Iron Centers in *Paracoccus halodenitrificans* Nitric Oxide Reductase

Takeshi SAKURAI, Nobuhiko SAKURAI, Hiroki MATSUMOTO (*Nagoya Univ.*) Shun HIROTA (*Nagoya Univ.*) and Osamu YAMAUCHI (*Nagoya Univ.*)

[*Biochem. Biophys. Res. Commun.* in press]

Reactions of *Paracoccus halodentrificans* nitric oxide reductase (NOR) containing four iron centers, a low spin heme *c*, a low spin heme *b*, a high spin heme *b* and a non-heme iron, have been studied to show the roles of each iron center. Soon after reacting the resting (oxidized) NOR with L-ascorbate the low spin heme *c* and low spin heme *b* were reduced to a considerable extent but the high spin heme *b* was still in the oxidized form and was reduced slowly. When CO was acted on the reduced NOR, the high spin heme *b* center changed to be a low spin state. On the other hand, when NO was acted on the resting NOR, no apparent spectral change was observed. However, when NO was acted on the reduced NOR (a steady state condition excess dithionite is present), both of the low spin centers changed to be partly in the oxidized form. A small but clear new EPR signal with $g = 4.1$ appeared together with some new signals at the $g = 2$ region soon after the action of NO on the reduced NOR. During incubation at room temperature the nitrosyl-heme signal typical of the 5-coordination developed. These results suggested that both of the high spin-heme *b* center and the non-heme iron are the reaction centers and their reductions are indispensable for the enzyme process in contrast to the reaction mechanism proposed for the P-450 type NOR (P-450nor).

VII-D-10 *Myrothecium verrucari* MT-1 Bilirubin Oxidase and Its Mutants for Potential Copper-Ligands

Atsushi SHIMIZU (*Aoyamagakuin Univ.*), Jung Hee KWON (*Aoyamagakuin Univ.*), Takashi SASAKI (*Aoyamagakuin Univ.*), Takanori SATOH (*Aoyama-gakuin Univ.*), Nobuhiko SAKURAI, Takeshi SAKURAI, Shotaro YAMAGUCHI (*Amano Pharm. Co.*) and Tatsuya SAMEJIMA (*Aoyamagakuin Univ.*)

[*Biochemistry* submitted]

Bilirubin oxidase [EC 1.3.3.5] which catalyzes the oxidation of bilirubin to biliverdin *in vitro* was purified from the culture medium of *Myrothecium verrucaria* MT-1 (authentic enzyme). The overexpression system of bilirubin oxidase gene was already established by using *Aspergillus oryzae* harboring an expression vector, thereby we obtained recombinant enzyme (wild type). The absorption and ESR spectra showed that the both bilirubin oxidases are a multicopper oxidase containing type 1, type 2, and type 3 coppers as similar with laccase, ascorbate oxidase, and ceruloplasmin. The cassette mutagenesis has been performed for the possible ligands of each type of coppers. In the mutants, Cys457 Val, Ala, His94 Val, and His134.136 Val, the type 1 and type 2 copper centers were perturbed completely and the enzyme activity was completely lost. And these mutants showed the ESR spectra differing from the holoenzyme, showing the type 3 copper signal. However, the optical and magnetic property characteristic for the type 1 copper was retained even by mutating one of the type 1 copper ligand, *i.e.*, the mutant, Met467 Gly, whose enzyme activity was also retained slightly. Furthermore, the mutant His456.458 Val completely lost the enzyme activity and characteristics for type 2 and type3 coppers but still retained the type 1 copper. These results support that these above amino acids as the copper ligands and the peculiar sequence in the multicopper oxidases, His-Cys-His, also appeared in bilirubin oxidase to form the intramolecular electron transfer pathway between the type 1 copper site and the trinuclear center composed of the type 2 and type 3 copper sites.

VII-E Homogeneous Catalysis with Novel Reactivity

Highly active and selective homogeneous catalytic systems are developed. Mechanistic studies are carried out with isolated active catalytic species and related model complexes.

VII-E-1 Palladium Complex Catalyzed Cyanation of Allylic Carbonates and Acetates Using Trimethylsilyl Cyanide

Yasushi TSUJI, Tomohito KUSUI (*Gifu Univ.*), Takaharu KOJIMA (*Gifu Univ.*), Yoshihiko SUGIURA (*Gifu Univ.*), Naoaki YAMADA (*Gifu Univ.*), Shinsuke TANAKA (*Gifu Univ.*), Masahiro EBIHARA (*Gifu Univ.*) and Takashi KAWAMURA (*Gifu Univ.*)

[*Organometallics* in press]

Allylic carbonates are cyanated in high yields to α,β -unsaturated carbonitriles using trimethylsilyl cyanide in the presence of catalytic amount (5 mol%) of Pd(PPh₃)₄

in THF under reflux. In the reaction, cinnamyl methyl carbonate affords cinnamyl cyanide in 98% yield. Allylic acetates also provide the corresponding carbonitriles, but often in lower yields. The cyanations of several *cis*- and *trans*-alicyclic substrates proceed cleanly (stereoselectivity > 99%) with overall retention. Characterization and reaction of palladium complexes relevant to the present catalysis indicate that transmetalation of α^3 -allyl palladium complex with trimethylsilyl cyanide is facile, while the resulting cyano(α^3 -allyl)palladium complexes afford the corresponding allylic cyanides only when excess trimethylsilyl cyanide is present. Stereochemistry of the product indicates that the CN attacks the α^3 -allyl moieties from the palladium side.

VII-F Bio-Inspired Molecular Architecture

Nature has produced a limited number of molecular modules such as nucleosides and nucleotides, amino acids, and lipids. However, the chemical diversity of these biomolecules and the different ways they can be polymerized or assembled into precisely-defined three-dimensional shapes provide a wide range of possible structures and functions. Furthermore, owing to advances in chemical synthesis and biotechnology we can combine or chemically modify these molecular building blocks, almost at will, to produce new functional molecules that have not yet been made in Nature. Based on these concepts, we have been working on the following research projects. Our research programs also consciously focus on structures and functions that have been unknown in living, biological systems.

VII-F-1 Double-Strands Formation of Artificial DNAs Induced by Metal Complexation

Kentaro TANAKA, Honghua CAO (*Grad. Univ. Adv. Stud.*), Motoyuki TASAKA (*Grad. Univ. Adv. Stud.*) and Mitsuhiko SHIONOYA

[*Nucleic Acids Res., Symp. Ser.* **39**, 171 (1998)]

An artificial DNA was synthesized, to which nonnatural bases were introduced as metal coordination sites, for the purpose of controlling higher-order structures of DNAs and for utilizing DNA as functionalized materials. The artificial DNA forms double stranded structure by metal complexation instead of hydrogen bonding in natural DNA. An artificial β -C-nucleoside **1** (Figure 1a) which has a phenylenediamine base as the metal coordination site was prepared by coupling reaction of lithiated *o*-phenylenediamine derivative and *O*-protected 1,4-ribonolactone followed by several steps to remove 2'-hydroxyl group. Figure 1b shows $^1\text{H-NMR}$ spectra of metal complex formation between C-nucleoside **1** and Pd^{2+} . The chemical shifts of the aromatic moiety shifted to lower field almost linearly with increasing concentration of Pd^{2+} until the concentration reached at a half of that for **1**. This result shows that **1** and Pd^{2+} form a stable 2:1 complex with a high binding constant. To control the number of charges of the metal complex moiety, the synthesis of new nucleobases bearing a catechol or an aminophenol as the nucleobase is now underway.

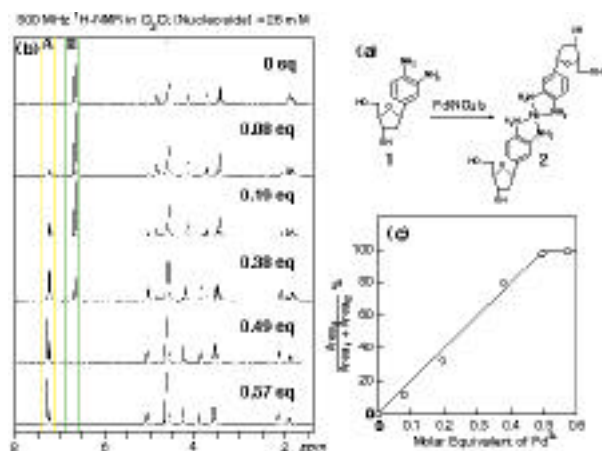


Figure 1. Complex formation of phenylenediamine-nucleoside with Pd^{2+} : (a) reaction scheme, (b) $^1\text{H-NMR}$ spectra of **1** with various concentrations of Pd^{2+} , (c) proportion of metal complex against molar equivalent of Pd^{2+} added.

VII-F-2 Metal-Assisted Formation of Artificial Nucleic Acids

Akihiko HATANO (*Grad. Univ. Adv. Stud.*), Hiromasa MORISHITA (*Grad. Univ. Adv. Stud.*), Kentaro TANAKA and Mitsuhiko SHIONOYA

[*Nucleic Acids Res., Symp. Ser.* **39**, 93 (1998)]

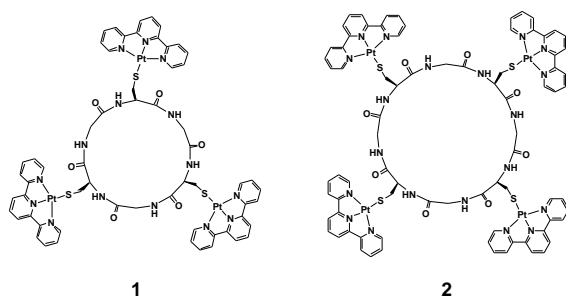
Self-assembly processes are used to create complex functional biological structures of nano scale dimensions with precision, and are now recognized as efficient tools in the construction of new systems with tailored functions. DNA, which is a genetic biomolecule, forms a double helical structure with two complementary single strands through hydrogen bonding, and stores genetic information. In this work, we have designed a self-assembling nucleic acid which could be built up by molecular subunits with the cooperative participation of metal coordination, hydrogen bonding, and hydrophobic interaction etc. The compound **1** we first prepared in this work has a thymine base moiety and two amino carboxylic acid subunits. This chelating compound **1** was expected to be aligned on an adenine-rich single stranded DNA (or RNA) through hydrogen bonding and metal coordination. The interactions between poly dA, the compound **1**, and metal ions (Mg^{2+} , Zn^{2+} , Mn^{2+} , Ni^{2+}) were examined by UV absorption changes around 260 nm. Effective interactions between these three components would result in a decrease in the absorption compared with the total absorption of each component. However, there was only a little absorption change in the presence of the above ions. The synthesis of **2**, in which the metal coordination sites of **1** are replaced by ethylene diamine subunits, is now in progress.



VII-F-3 An Efficient Strategy for the Liquid-Phase Synthesis of Cyclic Metallopeptides

Kazuki SHIGEMORI (*Grad. Univ. Adv. Stud.*),
Kentaro TANAKA and Mitsuhiro SHIONOYA

Synthetic cyclopeptides are interesting target molecules owing to their biological activity, their model character for enzymes or biomembranes, and their great potential as drugs and functional molecules such as nanotubes. New efficient synthetic methodology has been developed that can be utilized for the iterative construction of new families of cyclic metallopeptide oligomers of the general formula, cyclo[Gly-Cys(terpyPt^{II})]₃Cl₃, **1**, and cyclo[Gly-Cys(terpyPt^{II})]₄Cl₄, **2**. The linear peptides (Gly-L-Cys)_n trifluoroacetate salts (n = 3, 4) were synthesized on commercially available H-Cys(Trt)-2-ClTrt resin using standard Fmoc chemistry, cleaved from the solid support using trifluoroacetic acid in the presence of 1,2-ethanedithiol for the removal of triphenylmethyl groups from cystein residues, purified by RP-HPLC. [Gly-Cys(terpyPt^{II})]_n-Cl_n (n = 3, 4) were prepared from the above linear peptides and n eq [(terpy Pt^{II})Cl]Cl in H₂O at room temperature. The obtained linear metallopeptides were cyclized at 25°C in the presence of HOBt (10 mM) and EDC (100 mM) in H₂O-CH₃CN in high yields. A full analysis of these compounds by a variety of techniques, including UV-vis, ¹H NMR spectroscopies, electron spray mass, HPLC and capillary electrophoresis, has been performed. These cyclic metallopeptides proved to interact with DNA and cationic ions such as Mg²⁺, Ca²⁺, Gd³⁺, Tb³⁺, Eu³⁺ ions by circular dichroism spectroscopy.



VII-F-4 Highly Controlled and Hierarchical Assembly of Metal Complexes

Hiromasa MORISHITA (*Grad. Univ. Adv. Stud.*),
Xian-He BU (*Nankai Univ., China and IMS*), Kentaro
TANAKA and Mitsuhiro SHIONOYA

Biological materials assembly on a very broad range of organizational length scales, and in both hierarchical and nested manners. The concept of a hierarchy of structures of increasing size was referred to repeatedly, and comparisons were inevitably made with the organization of living manner. Self-assembly features the cooperative participation of non-covalent interactions to construct thermodynamically minimized structures. The main purpose of this research is to arrange functional molecular subunits on DNA by non-

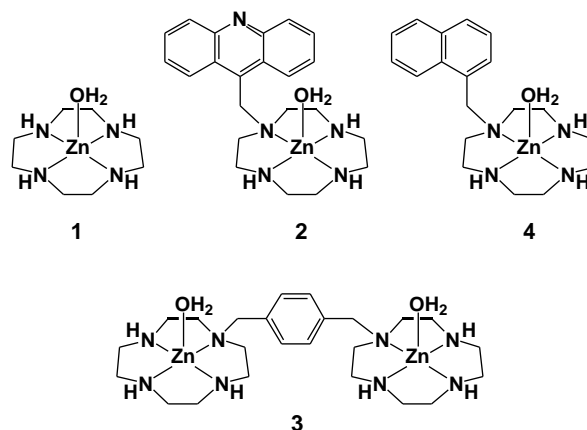
covalent interactions, or to array designed molecules in a hierarchical manner assisted by metal ions. We have synthesized new families of tetradentate ligands which can be linked to other two subunits through metal coordination.

VII-F-5 Macrocyclic Metal Complexes for Selective Recognition of Nucleic Acid Bases and Manipulation of Gene Expression

Eiichi KIMURA (*Hiroshima Univ.*), Takuya IKEDA
(*Hiroshima Univ.*) and Mitsuhiro SHIONOYA

[*Pure & Appl. Chem.* **69**, 2187 (1997)]

Interaction of Zn-cyclen complexes **1-4** with uracil and thymine bases in double-stranded poly(A)-poly(U) and poly(dA)-poly(dT) has been investigated. These zinc(II) complexes lowered the melting temperatures (*T_m*) of poly(A)-poly(U) and poly(dA)-poly(dT) in 5 mM Tris-HCl buffer (pH 7.6) containing 10 mM NaCl as their concentrations increased, indicating that they destabilized the duplex structure of polynucleotides. The comparison of CD spectra of poly(A)-poly(U), poly(A), and poly(U) in the presence of zinc(II) complex **2** led us to conclude that the spectral changes of poly(A)-poly(U) were due to a structural change from double to single-strand, caused by zinc(II) complex **2** binding exclusively to uracils in poly(U). The destabilization effect of the zinc(II) complexes was not observed on poly(dG)-poly(dC) in the thermal denaturation experiments in 50 % formamide aqueous solution containing 2.5 mM Tris-HCl buffer (pH 7.6) and 5 mM NaCl. However, the acridine-pendant cyclen complex **2**, which associates with guanine at N7 and O6, and through π -stacking, interacted with poly(dG) in the double helix to greatly stabilized the poly(dG)-poly(dC) double-strand, as was indicated by the higher *T_m* than those with reference intercalating agents. Poly(A)-poly(U) double-strand was most effectively broken with a bis(Zn-cyclen) bridged by para-xylyl group **3** that was designed as a host molecule to bind to two succeeding uracils in a 1:2 complex. Zn-cyclen complexes thus may become a prototype of small molecules that can affect the biological properties of nucleic acids at the molecular level.



VII-F-6 Macrocyclic Zinc(II) Complexes for Selective Recognition of Nucleobases in Single- and Double-Stranded Polynucleotides

Eiichi KIMURA (*Hiroshima Univ.*), Takuya IKEDA (*Hiroshima Univ.*), Mariko MURATA (*Hiroshima Univ.*) and Mitsuhiro SHIONOYA

[*J. Bioinorg. Chem.* **3**, 259 (1998)]

Interaction of a series of Zn-cyclen complexes, which selectively bind to thymine and uracil nucleosides in aqueous solution at physiological pH, with polynucleotides has been examined. These

complexes disrupt the A-U (or T) H-bonding to unzip the duplex of poly(A)-poly(U), as demonstrated by lowering melting temperatures of poly(A)-poly(U) and poly(dA)-poly(dT) with an increase in their concentrations. The order of the denaturing efficiency is well correlated with the order of the 1:1 affinity constants for each complex. The comparison of CD spectra of poly(A)-poly(U), poly(A), and poly(U) in the presence of the Zn-complex of acridine-pendant-cyclen revealed a structural change from poly(A)-poly(U) to single-stranded poly(A) and poly(U). This can be explained by the exclusive binding of this complex to uracils in poly(U). These Zn complexes, on the other hand, stabilized poly(dG)-poly(dC).

VII-G Stereochemistry of Coordination Compounds and Adsorption Phenomena of Various Gases on Inorganic Solids

Several coordination compounds including higher (than four)-coordinate silicon(IV) complexes are going to be synthesized and studied stereochemically and kinetically.

Dielectric properties of inorganic solids adsorbed water molecules, on which the two-dimensional condensation of water molecules occurs, were investigated as a function of surface coverage. Adsorption properties of dinitrogen (N_2) on copper-ion-exchanged mordenites were also investigated.

VII-G-1 Analysis of Active Sites on Copper Ion-Exchanged ZSM-5 for CO Adsorption through IR and Adsorption-Heat Measurements

Yasushige KURODA (*Okayama Univ.*), Yuzo YOSHIKAWA, Ryotaro KUMASHIRO (*Okayama Univ.*) and Mahiko NAGAO (*Okayama Univ.*)

[*J. Phys. Chem. B* **101**, 6497 (1997)]

The state of copper ion exchanged in ZSM-5-type zeolite has been investigated through the IR and adsorption-heat measurements at 301 K by using CO as a probe molecule. As a result, it was proved that there are at least three kinds of adsorption sites for a CO molecule on the copper ion-exchanged ZSM-5, which are responsible for the IR bands at 2159, 2149, and 2136 cm^{-1} , as well as the differential adsorption-heats of 91, 82, and ~ 70 $kJ mol^{-1}$. Corresponding to these data, TPD also gives three desorption peaks at 363, 442, and 542 K. An excellent linear relationship has been established between the stretching vibrational frequencies due to the adsorbed CO species and the differential adsorption-heat values. When a CO gas is introduced to the 723 K-treated sodium ion-exchanged ZSM-5, this sample provides the adsorption-heat of about 35 $kJ mol^{-1}$ in the whole adsorption region studied and the weak IR bands at 2175 and 2112 cm^{-1} . For the sodium ion-exchanged ZSM-5 and CO system, the above correlation does not hold in the same plot containing Cu-CO species. This fact is interpreted in terms of the difference in the nature of bonding between the electrostatic force for the sodium ion-exchanged ZSM-5 and CO system and the covalent nature for the copper ion-exchanged ZSM-5 and CO system. More detailed discussions are also made on the nature of Cu-

CO bond.

VII-G-2 Preparative Study and Characterization of the *Cis*-Diamminetetranitro-Cobaltate(III) Ion — A Missing Link in the Ammine-Nitro Cobalt(III) Series

Miho FUJITA (*Nagoya City Univ.*), Takashi FUJIHARA (*Saitama Univ.*), Masaaki KOJIMA (*Okayama Univ.*), Yuzo YOSHIKAWA and Kazuo YAMASAKI, M.J.A. (*Nagoya Univ.*)

[*Proc. Jpn. Acad.* **73B**, 161 (1997)]

The preparative conditions and stability of *cis*-[Co(NO₂)₄(NH₃)₂]⁻, which had been a missing link in the nitro-ammine cobalt(III) series until recently, was studied using cobalt-59 NMR spectroscopy. The reaction of Na₃[Co(NO₂)₆] with liquid ammonia mainly gave *cis*-[Co(NO₂)₄(NH₃)₂]⁻ together with *mer*- and *fac*-[Co(NO₂)₃(NH₃)₃] and *cis*-[Co(NO₂)₂(NH₃)₄]⁺; the formation of *trans*-[Co(NO₂)₄(NH₃)₂]⁻ was not observed. The reaction of aqueous [Co(NO₂)₆]³⁻ with aqueous ammonia also gave the *cis*-isomer as a major product. On the contrary, the *cis*-isomer did not form during the conventional preparation from CoCl₂ in an aqueous solution. The *cis*-isomer was very stable in the solid state, but the isomer slowly isomerized in water ($t_{1/2} > 5$ days at room temperature, *ca.* 0.1 mol/dm³) to the *trans*-isomer. The reaction was accompanied by the formation of *fac*-[Co(NO₂)₃(NH₃)₃] which then isomerized to the *mer*-isomer, and by the formation of several unknown species.

VII-G-3 Chromatographic Separation and Characterization of the Photoproduct of Tris(L-

cysteinesulfinato-*N,S*)cobaltate(III)Masaaki KOJIMA (*Okayama Univ.*) and Yuzo YOSHIKAWA[*J. Chromatogr. A* **789**, 273 (1997)]

The product of photolysis of $K_3 (+)-[Co(L-cysi-N,S)_3]$ (**1**, L-cysi = L-cysteinesulfinate(2-) ion, cysi = $NH_2CH(COO^-)CH_2SO_2^-$) was separated by column chromatography on DEAE-Sephadex A-25. The main band contained $[Co(L-cysi-N,S)_2(L-cysi-N,O)]^{3-}$ (**2**); linkage isomerization from sulfinato-*S* to sulfinato-*O* took place. This complex (**2**) is thermally unstable and reverts to the starting complex (**1**). An anion-exchange high-performance liquid chromatographic (HPLC) method was successfully applied to the kinetic study of this linkage isomerization reaction from **2** to **1**.

VII-G-4 Stereochemistry of (*R*)-2 Methyl Aziridine Complex of Cobalt(III) and Dimerization of the LigandMasaaki KOJIMA (*Okayama Univ.*), Akiko SAKURAI (*Okayama Univ.*), Mayumi MURATA (*Okayama Univ.*), Kiyohiko NAKAJIMA (*Aichi Univ. Educ.*), Setsuo KASHINO (*Okayama Univ.*) and Yuzo YOSHIKAWA[*J. Coord. Chem.* **42**, 95 (1997)]

A cobalt(III) complex containing (*R*)-2-methylaziridine (*R*-meaz), $[Co(R-meaz)(NH_3)_5]^{3+}$, was prepared and the two diastereomers arising from the presence of the chiral nitrogen atom (*N*(*R*) and *N*(*S*)) were separated by the column chromatographic method. Molecular mechanics calculations estimated the *N*(*R*)-isomer to be more stable. This result was supported by the X-ray structure determination of the more abundant (*ca.* 94%) isomer, *N*(*R*)- $[Co(R-meaz)(NH_3)_5]Br_3 \cdot H_2O$. Crystal data: monoclinic, $P2_1$, $a = 7.357(1)$, $b = 9.780(1)$, $c = 10.426(1)$ Å, $\beta = 93.58(1)^\circ$, $V = 748.7(3)$ Å³, $Z = 2$. Kinetic studies of isomerization (epimerization) between the two isomers revealed that the inversion at the nitrogen center was very slow ($5 \times 10^{-2} M^{-1} s^{-1}$ at 25 °C). The small rate constant seems to be related to the strained three-membered structure of the meaz ligand. The reaction of $Na_3[Co(NO_2)_6]$ and *R*-meaz yielded a complex containing two dimerized *R*-meaz chelates, $trans-[Co(NO_2)_2(di-R-meaz)_2]^+$ (*di-R-meaz* = (*RR*)-2-dimethyl-1-aziridineethanamine). The crystal structure of $trans-[Co(NO_2)_2(di-R-meaz)_2] \cdot ClO_4 \cdot H_2O$ was established by the X-ray method. Crystal data: orthorhombic, $P2_12_12_1$, $a = 11.784(6)$, $b = 21.023(9)$, $c = 8.608(7)$ Å, $V = 2133(2)$ Å³, $Z = 4$.

VII-G-5 Development of Site-Selective Copper-**Ion-Exchanging Method of HZSM-5 by the Vapourization of Hexafluoroacetylacetonato-Copper Complex**Yasushige KURODA (*Okayama Univ.*), Kazunori YAGI (*Okayama Univ.*), Yuzo YOSHIKAWA, Ryotaro KUMASHIRO (*Okayama Univ.*) and Mahiko NAGAO (*Okayama Univ.*)[*Chem. Comm.* 2241 (1997)]

The deposition of copper ion into one single ion-exchange site in HZSM-5-type zeolite was successful by using bis(1,1,1,5,5,5-hexafluoroacetylacetonato)-copper(II) as a volatile complex, and differing from the sample prepared by ion-exchanging operation, which gives a couple of bands at 2158 and 2151 cm^{-1} .

VII-G-6 A Stable Sulfonato-Cobalt(III) Complex: $-[Co\{OS(O)_2CH_2CH_2NH_2-N,O\}(en)_2\}(ClO_4)_2$ Mayumi MURATA (*Okayama Univ.*), Masaaki KOJIMA (*Okayama Univ.*), Masakazu KITA (*Naruto Univ.*), Setsuo KASHINO (*Okayama Univ.*) and Yuzo YOSHIKAWA[*Acta Cryst. C* **53**, 1761 (1997)]

A stable sulfonato complex, (2-aminoethane-sulfonato-*N,O*)bis(ethylenediamine-*N,N'*)cobalt(III) perchlorate, $[Co(C_2H_6NO_3S)(C_2H_8N_2)_2](ClO_4)_2$, was prepared by oxidation of $[Co\{OS(O)CH_2CH_2NH_2-N,O\}(en)_2]^{2+}$ ($en = NH_2CH_2CH_2NH_2$) in acid media. This sulfonato complex was resolved by SP-Sephadex column chromatography and the absolute configuration of the slower eluted ($-$)₅₈₉-isomer was determined by X-ray analysis to be .

VII-G-7 Complete Chromatographic Resolution of Axially Chiral β -Diketonate Complexes on Cellulofine C-200Yoshiharu NAKANO (*Ibaraki Univ.*), Takeshi KAWAGUCHI (*Ibaraki Univ.*) and Yuzo YOSHIKAWA[*J. Coord. Chem.* **43**, 219 (1998)]

New chromatography on Cellulofine C-200 (modified polysaccharide ion exchanger) completely resolved the atropisomers reported previously [2]. The present technique needs no optically active eluting agents, differing from conventional chromatography on SP-Sephadex. The chromatographed atropisomers, axially chiral β -diketonate cobalt(III)-tren complexes, are listed in the table in the text.

VII-H Syntheses of Transition Metal-Sulfur Clusters and Development of Their Catalysis

This project focuses on the development of the new, reliable synthetic pathways affording the transition metal-

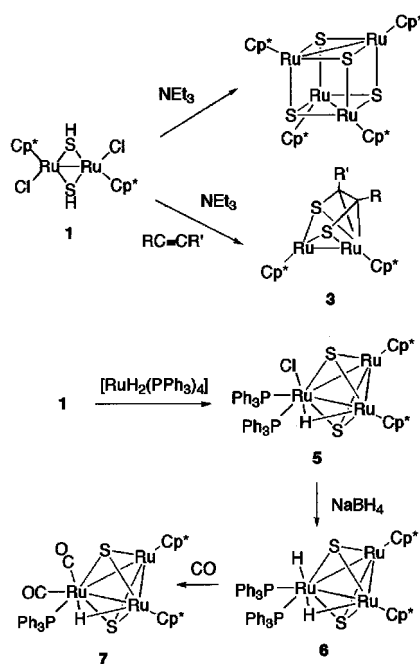
sulfur clusters with the tailored core structures in high yield, and also on the determination of the detailed structures of the novel clusters prepared in this study by the X-ray crystallography. Activation of the small molecules will be attempted by the use of polynuclear homo- or heterometallic site in these clusters to exploit the new catalytic reactions that are inaccessible by the mononuclear complex catalyst.

VII-H-1 Structures and Reactivities of Diruthenium Dithiolene Complexes and Triruthenium Sulfido Clusters Derived from a Hydrosulfido-Bridged Diruthenium Complex

Shigeki KUWATA (Univ. Tokyo), Masahiro ANDOU (Univ. Tokyo), Kohjiro HASHIZUME (Univ. Tokyo), Yasushi MIZOBE (Univ. Tokyo and IMS) and Masanobu HIDAI (Univ. Tokyo)

[Organometallics 17, 3429 (1998)]

The hydrosulfido-bridged diruthenium complex $[\text{Cp}^*\text{RuCl}(\mu_2\text{-SH})_2\text{RuClCp}^*]$ (**1**; $\text{Cp}^* = {}^5\text{-C}_5\text{Me}_5$) reacted with an excess of triethylamine to give the cubane-type tetra ruthenium sulfido cluster $[(\text{Cp}^*\text{Ru})_4(\mu_3\text{-S})_4]$ through dimerization of the coordinatively unsaturated species $[\text{Cp}^*\text{Ru}(\mu_2\text{-S})_2\text{RuCp}^*]$ (**2**) generated in situ. When the reaction was carried out in the presence of alkynes, **2** was trapped by the alkyne and the dithiolene-bridged diruthenium complexes $[(\text{Cp}^*\text{Ru})_2(\mu_2\text{-}^2\text{-}^4\text{-S}_2\text{C}_2\text{RR}')]$ (**3**) were obtained. Treatment of **3** with CO afforded the carbonyl complexes $[(\text{Cp}^*\text{Ru}(\text{CO})(\mu_2\text{-}^2\text{-}^4\text{-S}_2\text{C}_2\text{RR}')\text{RuCp}^*)]$ (**4**) containing a bent dithiolene ring. On the other hand, the reaction of **1** with an equimolar amount of $[\text{RuH}_2(\text{PPh}_3)_4]$ resulted in the formation of the triruthenium sulfido cluster $[(\text{Cp}^*\text{Ru})_2(\mu_3\text{-S})_2(\mu_2\text{-H})\text{RuCl}(\text{PPh}_3)_2]$ (**5**). Cluster **5** reacted with an excess of NaBH_4 in ethanol to give the dihydrido cluster $[(\text{Cp}^*\text{Ru})_2(\mu_3\text{-S})_2(\mu_2\text{-H})\text{RuH}(\text{PPh}_3)_2]$ (**6**), which was further converted to the dicarbonyl cluster $[(\text{Cp}^*\text{Ru})_2(\mu_3\text{-S})_2\text{Ru}(\text{CO})_2(\text{PPh}_3)]$ (**7**) under CO. The structures have been determined in detail by the X-ray analyses for the new compounds, **3a** ($\text{R} = \text{H}$, $\text{R}' = \text{Bu}^t$), **4a** ($\text{R} = \text{H}$, $\text{R}' = \text{Bu}^t$), **5**, **6**, and **7**.

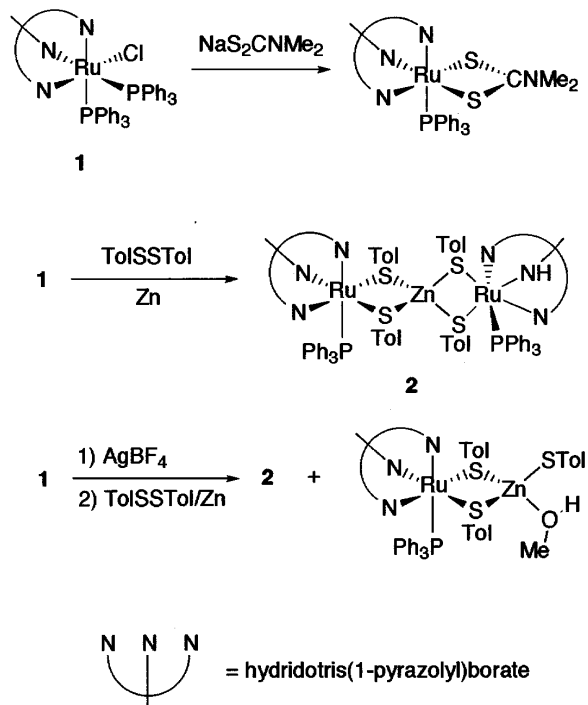


VII-H-2 Syntheses of Ruthenium Hydridotris(1-pyrazolyl)borate Complexes Having Sulfur-Donor Coligands

Yasushi MIZOBE (Univ. Tokyo and IMS), Masayuki HOSOMIZU (Univ. Tokyo) and Masanobu HIDAI (Univ. Tokyo)

[Inorg. Chim. Acta 273, 238 (1998)]

Treatment of $[\text{TpRuCl}(\text{PPh}_3)_2]$ (**1**; Tp = hydridotris(1-pyrazolyl)borate) with $\text{NaS}_2\text{CNMe}_2$ afforded the dithiocarbamate complex $[\text{TpRu}(\mu_2\text{-S}_2\text{CNMe}_2)(\text{PPh}_3)]$ in high yield, whose structure has been determined by the X-ray diffraction study. Complex **1** also reacted with a mixture of excess TolSSTol (Tol = *p*- MeC_6H_4) and Zn powder to give a novel trinuclear complex with bridging thiolate ligands $[\{\text{TpRu}(\text{PPh}_3)(\mu\text{-STol})_2\}_2\text{Zn}]$ (**2**) in moderate yield, which has been characterized spectroscopically and by elemental analysis. Initial treatment of **1** with an equimolar amount of AgBF_4 followed by the reaction with a mixture of TolSSTol and Zn also resulted in the formation of **2** as the major product. However, from this reaction mixture, a dinuclear complex closely related to **2**, $[\text{TpRu}(\text{PPh}_3)(\mu\text{-STol})_2\text{Zn}(\text{STol})(\text{MeOH})]$, was able to be isolated in quite a low yield, which has been fully characterized by the X-ray analysis.



VII-H-3 Unprecedented Conversion of Benzylideneanilines into Aryl Isocyanides Promoted by a Low-Valent Molybdenum Complex. X-Ray Structure of *trans*- $[\text{Mo}(\text{CNPh})_2]$

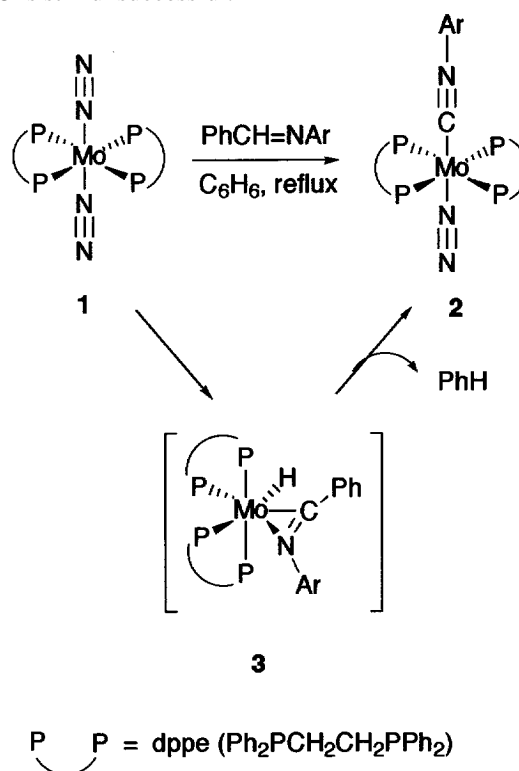
(N₂)(Ph₂PCH₂CH₂PPh₂)₂

Goh NAKAMURA (*Univ. Tokyo*), **Yuji HARADA** (*Univ. Tokyo*), **Chirima ARITA** (*Univ. Tokyo*), **Hidetake SEINO** (*Univ. Tokyo*), **Yasushi MIZOBE** (*Univ. Tokyo and IMS*) and **Masanobu HIDAI** (*Univ. Tokyo*)

[*Organometallics* **17**, 1010 (1998)]

The molybdenum dinitrogen complex *trans*-[Mo(N₂)₂(dppe)₂] (**1**; dppe = Ph₂PCH₂CH₂PPh₂) reacts with an excess of PhCH=NAr (Ar = Ph, *p*-MeC₆H₄, *p*-MeOC₆H₄) in benzene at reflux under N₂ to give novel isocyanide-dinitrogen complexes *trans*-[Mo(CNAr)(N₂)(dppe)₂] (**2**) in moderate yield. The concurrent formation of benzene by the cleavage of the benzyldiene C—Ph and C—H bonds have been confirmed by the GLC analysis of the reaction mixtures of **1** with PhCH=NAr (Ar = Ph, C₆H₄Me-*p*) in toluene or xylene. An X-ray diffraction study of **2** (Ar = Ph) has unambiguously disclosed the essentially linear Mo—C—N and C—N—C linkages in the PhNC ligand, which is *trans* to the N₂ ligand bound to the Mo atom in an end-on fashion. The reaction presumably proceeds via the iminoacyl species **3** as the key intermediate, which is formed by the oxidative addition of the benzyldiene C—H bond to the coordinatively unsaturated, low-valent Mo center generated in situ

from **1** upon thermolysis, although isolation or detection of **3** is still unsuccessful.



VII-I Activation of Carbon Dioxide and Energy Conversion from Proton Gradients to Electricity Mediated by Metal Complexes

An electrophilic attack of CO₂ to coordinatively unsaturated metal complexes produces M⁻¹-CO₂ complexes, which can be converted to M-CO complexes as precursors to CO evolution. Metal complexes with a chelate ring that has an ability of ring-opening and -closing in a catalytic cycle of reduction of CO₂ would largely contribute to the increment of thermal stability of low-valent coordinatively unsaturated metal complexes. Metal complexes used as homogeneous catalysts in the reduction of CO₂ have been desired to have a function of smooth CO evolution under mild conditions. On the other hand, reduction of M-CO bonds with depression of CO evolution in the reduction of CO₂ is expected to enable multi-electron reduction of CO₂ catalyzed by metal complexes. Thus, designing of molecular catalysts which have an ability of smooth conversion from CO₂ to CO without reductive cleavage metal-CO bonds would lead to new methodology for multi-electron reduction of CO₂ with carbon-carbon bond formation.

Biological system utilizes proton gradient for synthesis of ATP. The proton gradient (Δp) between inside and outside of a cell is depicted as the sum of electric activity ($\Delta \psi$) and chemical activity (ΔpH) components. $\Delta p = \Delta \psi - Z \Delta \text{pH}$ ($Z = 2.303RT/F$). When we are concerned about chemical activity part, proton gradient is equivalent to the neutralization energy because the neutralization reaction takes place if the separating membrane is removed. Biological system creates various valuable energies from the neutralization, which, however, is just emitted as thermal energy on the disposition of waste acids or bases in industrial process. Basically, neutralization energy is originated from the binding energy of acid and base, namely is one of the chemical energies, which are able to be converted directly to valuable chemical, electric or mechanical energy in 100% efficiency in principle. Along this line, we tried to convert the neutral energy to electronic energy by using ruthenium-aqua complexes.

VII-I-1 Catalytic Generation of Oxalate through Activation of Two CO₂ Molecules on [(IrCp*)₂(Ir-⁴-Cp*CH₂CN)(μ₃-S)₂]

Koji TANAKA, **Yoshinori KUSHI**, **Kiyoshi TSUGE**, **Kiyotsuna TOYOHARA**, **Takanori NISHIOKA** and **Kiyoshi ISOBE**

[*Inorg. Chem.* **37**, 120 (1998)]

Electrochemical reduction of CO₂ in the presence of [(IrCp*)₃(μ₃-S)₂](BPh₄)₂ [(Ir₃S₂](BPh₄)₂) in CH₃CN at -1.30 V (vs. Ag/AgCl) produced C₂O₄²⁻ with a current efficiency of 60%, and [(IrCp*)₂(Ir-⁴-Cp*CH₂CN)(μ₃-S)₂]⁺ [(Ir₃S₂CH₂CN)⁺] was isolated from the electrolyte

solution. Crystal structure of $[\text{Ir}_3\text{S}_2\text{CH}_2\text{CN}](\text{BPh}_4)$ by X-ray analysis revealed that a linear CH_2CN group is linked at the exo-position of a C_p^* ligand, and the $\text{C}_p^*\text{CH}_2\text{CN}$ group coordinates to an Ir atom with an η^4 -mode. The cyclic voltammogram of $[\text{Ir}_3\text{S}_2\text{CH}_2\text{CN}]^+$ in CH_3CN under CO_2 exhibited a strong catalytic current due to the reduction of CO_2 , while that of $[\text{Ir}_3\text{S}_2]^{2+}$ did not show an interaction with CO_2 in the same solvent. Thus, the reduced form of $[\text{Ir}_3\text{S}_2\text{CH}_2\text{CN}]^+$ works as the active species in the reduction of CO_2 . The IR spectra of $[\text{Ir}_3\text{S}_2\text{CH}_2\text{CN}]^+$ in CD_3CN showed a reversible adduct formation with CO_2 . The controlled potential electrolysis of $[\text{Ir}_3\text{S}_2\text{CH}_2\text{CN}]^+$ at -1.50 V under CO_2 evidenced the generation of $\text{C}_2\text{O}_4^{2-}$ through a 1:2 adduct between $[\text{Ir}_3\text{S}_2\text{CH}_2\text{CN}]^0$ and CO_2 . A coupling reaction of two CO_2 molecules activated on adjacent μ_3 -S and Ir in $[\text{Ir}_3\text{S}_2\text{CH}_2\text{CN}]^0$ is proposed for the first selective generation of $\text{C}_2\text{O}_4^{2-}$.

VII-1-2 Selective formation of HCOO^- and $\text{C}_2\text{O}_4^{2-}$ in Electrochemical Reduction of CO_2 Catalyzed by Mono- and Dinuclear Ruthenium Complexes

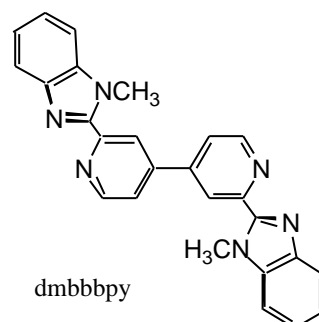
Md. Meser ALI (*Mie Univ.*), Hiroyasu SATO (*Mie Univ.*), Tetsunori MIZUKAWA, Kiyoshi TSUGE, Masa-aki HAGA and Koji TANAKA

[*J. Chem. Soc., Chem. Commun.* 249 (1998)]

A key process for the activation of CO_2 on metals is how to create coordinatively unsaturated low valent metal centers under mild conditions. The first catalytic oxalate formation in the reduction of CO_2 catalyzed by $[(\text{CpM})_3(\mu_3\text{-S})_2]^{2+}$ ($\text{M} = \text{Co}, \text{Rh}, \text{Ir}$) is ascribed to creation of the reaction sites by an M-M bond cleavage upon the two electron reduction of these M_3S_2 clusters. Metal complexes with unsymmetrical chelating rings may also provide sites for activation of CO_2 by dechelation in the electrochemical reduction of CO_2 . We introduced 2,2'-bis(1-methylbenzimidazo-2-yl)-4,4'-bipyridine (dm bbbbpy) as an unsymmetrical chelating ligand into a $\text{Ru}(\text{bpy})_2$ moiety to aim not only creation of reaction sites by opening of the chelate ring but also accumulation of electrons into the ligand required in the reduction of CO_2 . Indeed, electrochemical reduction of carbon dioxide catalyzed by mono- and dinuclear ruthenium complexes produced HCOOH with a trace amount of CO and $\text{C}_2\text{O}_4^{2-}$ in the presence and absence of H_2O , respectively, in CH_3CN .

$[\text{Ru}(\text{bpy})_2(\text{dm}\text{bbbbpy})](\text{PF}_6)_2$ (**1**) and dinuclear $[(\text{bpy})_2\text{Ru}(\text{dm}\text{bbbbpy})\text{Ru}(\text{bpy})_2](\text{PF}_6)_4$ (**2**) were synthesized by the reaction of $\text{Ru}(\text{bpy})_2\text{Cl}_2$ with dm bbbbpy with mole ratios of 1:1 and 2:1 respectively in ethyleneglycol. The controlled potential electrolysis of **1** and **2** (0.2-0.3 mmol/dm 3) at -1.65 and -1.55 V (vs Ag/AgCl) was conducted in CO_2 saturated CH_3CN (20 ml) in the presence of H_2O (0.5 ml). After 80 C was passed in the electrolysis of **1**, HCOO^- was produced with a current efficiencies (η) of 90% together with a trace amount of CO ($\eta = 2\sim 3\%$). On the other hand, the similar electrochemical reduction of CO_2 in dry CH_3CN selectively produced oxalate with an η of 60% without forming HCOO^- and CO after 90 C was passed in the

electrolysis. The electrochemical reduction of CO_2 catalyzed by **2** also generated almost selectively HCOO^- ($\eta = 90\%$) and $\text{C}_2\text{O}_4^{2-}$ ($\eta = 70\%$) in the presence and the absence of H_2O , respectively, under the similar conditions.

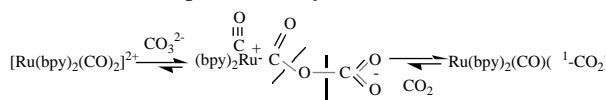


VII-1-3 Stabilization of $[\text{Ru}(\text{bpy})_2(\text{CO})(^1\text{-CO}_2)]$ and Unprecedented Reversible Oxide Transfer Reactions from CO_3^{2-} to $[\text{Ru}(\text{bpy})_2(\text{CO})_2]^{2+}$ and from $[\text{Ru}(\text{bpy})_2(\text{CO})(^1\text{-CO}_2)]$ to CO_2

Hiroshi NAKAJIMA, Kiyoshi TSUGE, Kiyotsuna TOYOHARA and Koji TANAKA

[*J. Organometallic Chem.* 569, 61 (1998)]

Metal complexes with an $^1\text{-CO}_2$ group are generally considered to be extremely labile to air, moisture and temperature. Thermal stability of metal- $^1\text{-CO}_2$ bonds will be improved by an increase of an electron donor ability of central metals, since a metal- $^1\text{-CO}_2$ bond is formed by overlap of the filled $\text{d}z^2$ orbital of d^8 metals and the empty CO_2^* orbital. Unusual thermal stability of $[\text{Ru}(\text{bpy})_2(\text{CO})(^1\text{-CO}_2)]$ (**1**) as a metal- $^1\text{-CO}_2$ complex was examined both in the solid state and in solutions. **1** dissolves in CH_3CN containing LiCF_3SO_3 . Interaction between Li^+ and the $^1\text{-CO}_2$ group enhances an electron flow from Ru to the CO_2 ligand and greatly contributes to the stabilization of the Ru- $^1\text{-CO}_2$ bond. The reaction of $[\text{Ru}(\text{bpy})_2(\text{CO})_2](\text{PF}_6)_2$ with $[\text{Crown-K}]_2\text{CO}_3$ in dry CH_3CN selectively produced **1** through the 1:1 adduct with the $\text{RuC}(\text{O})\text{-OCO}_2$ moiety. Stoichiometric formation of **1** from the 1:1 adduct is also assisted by $[\text{Crown.K}]^+$ as a Lewis acid. Similarly, the reaction of $[\text{Ru}(\text{bpy})_2(\text{CO})_2](\text{PF}_6)_2$ with $(\text{Me}_4\text{N})_2\text{CO}_3$ in DMSO gave the 1:1 adduct in the initial stage, which gradually changed to a metalloanhydride complex, $[\text{Ru}(\text{bpy})_2(\text{CO})((\text{CO})_2\text{O})]$ due to the absence of Lewis acids to stabilize **1**, since an addition of LiCF_3SO_3 to the solution gave $[\text{Ru}(\text{bpy})_2(\text{CO})(^1\text{-CO}_2)]$ quantitatively.



VII-1-4 Synthesis and Characterization of Ruthenium Terpyridine Dioxolene Complexes: Resonance Equilibrium between Ru^{III} -Catechol and Ru^{II} -Semiquinone Forms

Masato KURIHARA, Stephane DANIELE, Kiyoshi

TSUGE, Hideki SUGIMOTO and Koji TANAKA

[*Bull. Chem. Soc. Jap.* **71**, 867 (1998)]

A series of [RuX(dioxolene)(terpy)] (terpy = terpyridine; X = Cl, OAc) and one-electron oxidized complexes were prepared. The molecular structures of [RuCl(O₂C₆H₂-3,5-Bu₂)(terpy)] (**1**) and [Ru(OAc)(O₂C₆H₄)(terpy)] (**3**) were determined by X-ray crystallography. Crystal data for **1**: monoclinic, space group *P2₁/c*, *Z* = 8, *a* = 11.548(1) Å, *b* = 18.224(5) Å, *c* = 30.002(8) Å, β = 96.51(2)°, and *R* = 0.077 (*R_w* = 0.068). Crystal data for **3**: monoclinic, space group *C₂/c*, *Z* = 8, *a* = 13.355(5) Å, *b* = 12.131(4) Å, *c* = 26.645(4) Å, β = 92.46(2)°, and *R* = 0.041 (*R_w* = 0.041). Although the binding mode of O₂C₆H₂-3,5-Bu₂ to Ru was not determined by the molecular structure of **1**, the carbon-oxygen and carbon-carbon bond lengths of O₂C₆H₄ in **3** were consistent with those of catecholato ligands. Electronic absorption spectra of [RuX(dioxolene)(terpy)] were explained by the electronic structure of [Ru^{II}X(semiquinone)(terpy)] rather than [Ru^{III}X(catecholato)(terpy)], while the reverse assignment was deduced from the IR spectra. Moreover, ESR spectra showed hyper-fine structures due to contribution of semiquinone superimposed on an axial pattern of the Ru(III) center indicating a resonance equilibrium between [Ru^{II}X(semiquinone)(terpy)] and [RuX(dioxolene)(terpy)].

VII-I-5 Novel Intramolecular Rearrangement of Hepta-Coordinate Rhenium(V) Complex with Catecholato and Terpyridine Ligands

Hideki SUGIMOTO, Kiyoshi TSUGE and Koji TANAKA

[*Chem. Lett.* 719 (1998)]

An addition of ReCl₃(tpy) to a methanol solution containing 3,6-di-tert-butyl-catechol and triethylamine gave a clear blue-black solution. After exposure of the solution to air at room temperature and then the addition of NH₄PF₆ to the solution resulted in precipitation of [Re(tpy)(diBucat)₂]PF₆·CH₃CN (**1**)PF₆·CH₃CN.

The ¹H NMR spectra of [**1**]⁺ in CD₂Cl₂ reveal fluctuation of the catecholato ligands. Aromatic protons of two diBucat ligands emerge as two sharp singlet signals (δ = 6.98 and 6.67 ppm) at -20 °C. Despite the non-equivalence of 4,5-protons of diBucat containing O(1) and O(2), the appearance of the singlet signal is probably caused by an incidental agreement of the chemical shifts of the two protons. The two singlets broaden with increasing temperatures, and coalesced to one broad signals at 50 °C. On the other hand, no fluctuation was observed in the proton signals of tpy in the temperature range. Such characteristic behavior of the proton signals of the diBucat and tpy ligands of [**1**]⁺ is explained by the exchange of O(3) and O(1) in the equatorial position between two diBucat ligands. This is the first example of dynamic behavior between two mono-capped trigonal prism structures of hepta-coordinate metal complexes. Detailed thermodynamic behavior and parameters will be discussed in elsewhere.

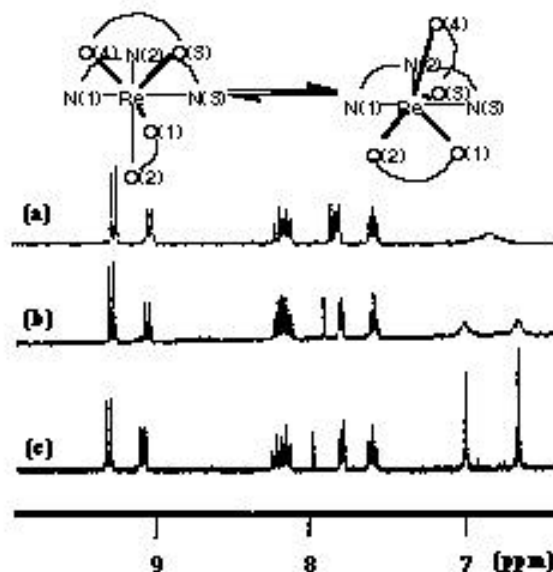


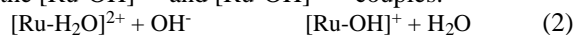
Figure 1. Temperature Dependent ¹H NMR spectra of the complex [**1**]⁺ in CD₂Cl₂; (a) 50°C, (b) 30°C, (c) -20°C.

VII-I-6 First Artificial Energy Conversion from Proton Gradient to Electricity

Kiyoshi TSUGE and Koji TANAKA

[*Chem. Lett.* 1069 (1998)]

Metal-aqua complexes are representative candidates for accumulation of proton gradient energy because they are expected to be converted to the corresponding hydroxy- and oxo-complexes by acid-base equilibria (eq 1), and the redox potentials of complexes change as [M(H₂O)] \rightleftharpoons [M(OH)]⁻ \rightleftharpoons [M(O)]²⁻ (1) release of protons. We prepared the ruthenium-aqua complex having a redox active quinone ligand, [Ru(tpy)(3,5-di-tert-butylquinone)(H₂O)]²⁺ ([Ru-H₂O]²⁺) to avoid dimerization and polymerization of hydroxy- and oxo complexes. The cyclic voltammogram (CV) of [Ru-H₂O]²⁺ in acetone. [Ru-H₂O]²⁺ undergoes two reversible redox couples at *E*_{1/2} = -0.47 V and *E*_{1/2} = 0.38 V (*E*_{1/2} = (*E*_{pc} + *E*_{pa})/2), which are assigned to the [Ru-H₂O]^{0/+} and [Ru-H₂O]⁺²⁺ couples, respectively. When 0.7 equivalent of OH⁻ was added to the solution, the rest potential of the solution (*V*_{rest}) shifted from 0.60 V to 0.30 V across the *E*_{1/2} of the [Ru-H₂O]⁺²⁺ couple (Figure 1b). At the same time, new redox couples appeared at *E*_{1/2} = -0.80 V and 0.00 V assignable to the [Ru-OH]^{0/+} and [Ru-OH]⁺²⁺ couples.



Further addition of OH⁻ caused deprotonation of [Ru-OH]²⁺ to produce [Ru-O] (eq 4), which equilibrates with the reactant (eq 5).



These redox reactions of this ruthenium aqua complex coupled with acid-base reactions enable the energy conversion from proton gradient to electricity. The energy conversion was conducted with two compartment cells (I and II) separated by an anion exchange membrane filled with an acetone solution of

$[\text{Ru-H}_2\text{O}]^{2+}$ (7.0 mmol/15 ml in each cell). Upon an addition of 1.6 equivalent of OH^- to cell(I), $[\text{Ru-H}_2\text{O}]^+$ and $[\text{Ru-OH}]^+$ formed and V_{rest} shifted from 0.60 V to -0.13 V (eqs 2-5). The connection of two cells induced current flow from the cell(II) to cell(I). At the end of the discharge (12 hr later), V_{rest} of two cells were 0.33 ± 0.02 V, and 0.50 C of electricity was obtained. Because the only difference between two cells is the amount of OH^- , pH gradient produces electric energy with this complex. Thus the proton gradient is catalytically converted to electricity by ruthenium aqua complex $[\text{Ru}(\text{trpy})(3,5\text{-di-tert-butylquinone})(\text{H}_2\text{O})]^{2+}$. The first successful energy conversion from proton gradient to electricity is based on the redox reactions of this ruthenium complex coupled with acid-base reaction.

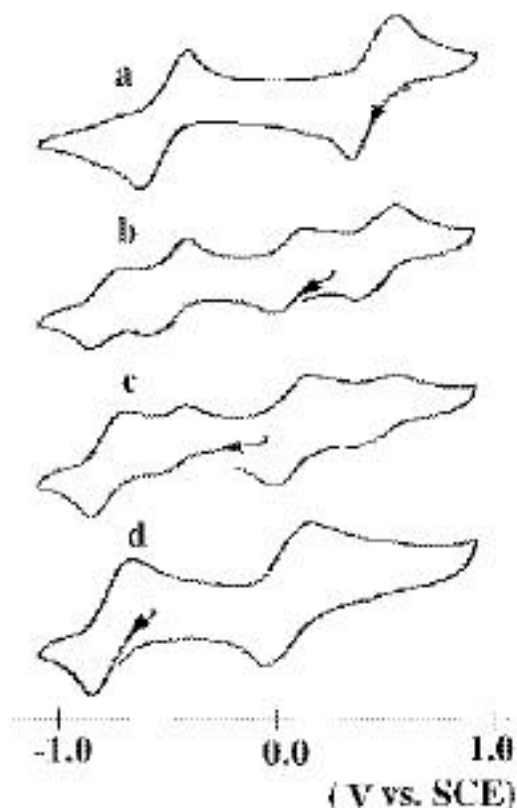


Figure 1. CV of $[\text{Ru}(\text{H}_2\text{O})]^{2+}$ (a) in the presence of 0 (a), 0.7 (b), 1.3 (c) and 2.0 (d) equiv of OH^- in acetone.

VII-I-7 Two-Electron Reduction of $\{[(\text{bpy})_2\text{Ru}(\text{dmbbbpy})]_3\text{Ru}\}^{8+}$ from $(\text{BNA})_2$ via Photoinduced Electron Transfer [dmbbbpy = 2,2'-Bis-(N-methylbenzimidazole-2-yl)-4,4'-bipyridine]

Md. Meser ALI (*Mie Univ.*), **Hiroyasu SATO** (*Mie Univ.*), **Koji TANAKA**, **Masa-aki HAGA**, **Akio YOSHIMURA** (*Osaka Univ.*) and **Takeshi OHNO** (*Osaka Univ.*)

[*Inorg. Chem.* in press]

Photoirradiation ($\lambda > 500$ nm) of $\{[(\text{bpy})_2\text{Ru}(\text{dmbbbpy})]_3\text{Ru}\}^{8+}$ ($\mathbf{1}^{8+}$) (dmbbbpy = 2,2'-Bis(N-methylbenzimidazole-2-yl)-4,4'-bipyridine and bpy = 2,2'-bipyridine) in the presence of dimeric N-benzylidihydronicotinamide, $(\text{BNA})_2$ produced stable

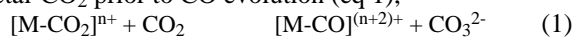
two-electron reduced species ($\mathbf{1}^{6+}$). Laser flash photolysis and emission spectroscopy were used to understand the reductive reaction pathways. The emission quenching k_q value ($4.1 \times 10^9 \text{ M}^{-1}\text{s}^{-1}$) obtained from Stern-Volmer plot is in excellent agreement with the electron transfer rate constant, k_{et} ($4.7 \times 10^9 \text{ M}^{-1}\text{s}^{-1}$) determined from the decay kinetics of transient ${}^3\mathbf{1}^{8+}$ triplet-triplet absorption at 650 nm indicating that photoreduction of $\mathbf{1}^{8+}$ proceeds via photoinduced electron transfer from $(\text{BNA})_2$ to ${}^3\mathbf{1}^{8+}$. After bimolecular electron transfer process, $\mathbf{1}^{8+}$ was reduced to $\mathbf{1}^{7+}$ and electron donor $(\text{BNA})_2$ was oxidized. Oxidation of $(\text{BNA})_2$ leads to the formation of highly reactive species, BNA^\cdot which then reduces $\mathbf{1}^{7+}$ to $\mathbf{1}^{6+}$. The quantum yield for the formation of the photo-reduction product was 0.026.

VII-I-8 Selective Production of Acetone in Electrochemical Reduction of CO_2 Catalyzed by Ru-Naphthyridine Complex

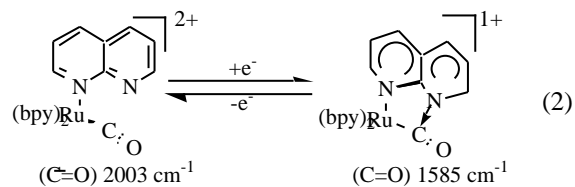
Tetsunori MIZUKAWA, **Kiyoshi TSUGE**, **Hiroshi NAKAJIMA** and **Koji TANAKA**

[*Angew. Chem.* in press]

Metal catalyzed reductive disproportionation of CO_2 proceeds through oxide transfer from metal- CO_2 to CO_2 followed by reductive cleavage of the resultant metal-CO bond. Acylation of the metal-CO bond derived from metal- CO_2 prior to CO evolution (eq 1),



therefore, leads to new methodology for carbon-carbon bond formation in the reduction of CO_2 . Polypyridyl ruthenium carbonyl complexes such as $[\text{Ru}(\text{bpy})_2(\text{quinoline})(\text{CO})]^{2+}$ and $[\text{Ru}(\text{bpy})(\text{terpyridine})(\text{CO})]^{2+}$ work as catalysts for the reduction of CO_2 of eq 1, and one electron reduction of these complexes causes bathochromic shift of their (CO) bands about by 30 - 40 cm^{-1} . The mono naphthyridine complex, $[\text{Ru}(\text{bpy})_2(\text{napy})(\text{CO})](\text{PF}_6)_2$ ($\mathbf{1}$) (napy = 1,8-naphthyridine- N), undergoes pronounced bathochromic shift of the $\nu(\text{CO})$ band ($\nu = 418 \text{ cm}^{-1}$) upon one-electron reduction due to a nucleophilic attack of the non-bonded nitrogen of monodentate napy to the carbonyl carbon (eq2).



Such metallacyclization would suppress the reductive cleavage of the Ru-CO bond (CO evolution), and enable reduction of the CO group derived from CO_2 .

Only CO and Li_2CO_3 were produced in the controlled potential electrolysis of $\mathbf{2}$ (0.6 mmol dm^{-3}) at -1.65 V (vs. Ag/Ag^+) with a glassy carbon (GC) electrode (4 cm^2) in CO_2 -saturated DMSO (30 cm^3) containing LiBF_4 (0.1 mol dm^{-3}) as an electrolyte. On the other hand, when $(\text{CH}_3)_4\text{NBF}_4$ was used as an electrolyte under otherwise the same conditions, $\text{CH}_3\text{C}(\text{O})\text{CH}_3$ was selectively generated with a trace amount

of CO. Besides these products, $(\text{CH}_3)_3\text{N}$ and $\{(\text{CH}_3)_4\text{N}\}_2\text{CO}_3$ were formed and no other product was detected in the solution. Thus, $(\text{CH}_3)_4\text{N}^+$ works as not only an electrolyte but also a methylation reagent for the catalytic generation of acetone in the electrochemical reduction of CO_2 catalyzed by **2** (eq 3). Based on the stoichiometry of eq 3, the current

$$2\text{CO}_2 + 4e^- + 2(\text{CH}_3)_4\text{N}^+ \rightarrow \text{CH}_3\text{C}(\text{O})\text{CH}_3 + \text{CO}_3^{2-} + 2(\text{CH}_3)_3\text{N} \quad (3)$$

efficiency of acetone was 70% at 100 C (turnover number 8.5) and that of CO was less than 1%.

VII-I-9 Basicity of μ_3 -X and 1 -Y Ligands (X, Y = S, Se) of Reduced, Oxidized and Super-Oxidized Forms of $[\text{Fe}_4\text{X}_4(\text{YAd})_4]^{2-}$ (Ad = 1-adamantane) in Aqueous Solutions

Masami NAKAMOTO, Kenji FUKAISHI, Tsuyoshi TAGATA, Hide KAMBAYASHI and Koji TANAKA

A series of $[\text{Fe}_4\text{X}_4(\text{YAd})_4]^{2-}$ (X, Y = S, Se; Ad = 1-adamantane) were prepared as a model of high potential

iron-sulfur proteins. Hydrolysis of those clusters were efficiently depressed in aqueous poly[2-dimethylamino-(hexanamide)] (PDAH) solutions due to the embedding effect in hydrophobic environment and/or inhibition of dissociation of the terminal ligand into the aqueous media. Cyclic voltammetry of the clusters in aqueous PDAH solutions showed pH dependent redox potentials of not only $[\text{Fe}_4\text{X}_4]^{+/2+}$ but also $[\text{Fe}_4\text{X}_4]^{2+/3+}$ (X, Y = S and Se) couples, resulting from redox-linked protonation reactions of three oxidation states of $[\text{Fe}_4\text{X}_4(\text{YAd})_4]^{n-}$ ($n = 1-3$). pK Values of the reduced, oxidized, and super-oxidized forms of $[\text{Fe}_4\text{X}_4(\text{YAd})_4]^{2-}$ were determined by computer simulation of the pH dependent redox potentials. The basicity of the μ_3 -X cores (X = S and Se) of three oxidation states of $[\text{Fe}_4\text{X}_4(\text{YAd})_4]^{n-}$ ($n = 1, 2, 3$) is stronger than the YAd (Y = S and Se) ligands: in the case of the mono-protonated $[\text{Fe}_4\text{X}_4(\text{YAd})_4]^{3-(\text{H}^+)}$ and $[\text{Fe}_4\text{X}_4(\text{YAd})_4]^{2-(\text{H}^+)}$, basicity of the 1 -Y ligand of $[\text{Fe}_4\text{X}_4(\text{YAd})_4]^{2-(\text{H}^+)}$ becomes stronger than that of μ_3 -X cores, although the μ_3 -X cores of $[\text{Fe}_4\text{X}_4(\text{YAd})_4]^{3-(\text{H}^+)}$ still show stronger basicity compared with those of 1 -Y ligands.

VII-J Supramolecular Self-Assembly through Coordination

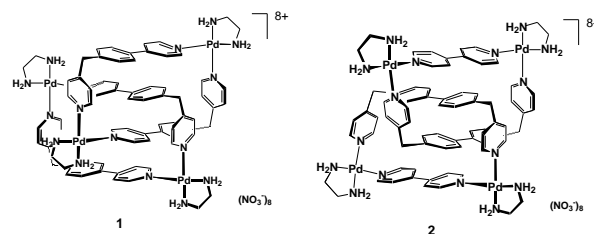
Supramolecular self-assembly refers to the spontaneous generation of well-defined structures from component molecules under a well-defined set of conditions. Since 1990, we have been studying the self-assembly of finite and infinite structures based on coordination chemistry, where coordinate bonds induce the generation of defined structures. Our studies are focused on the self-assembly of such finite structures as macrocycles, catenanes (interlocked molecules), and cages, as well as infinite network structures. In the construction of the discrete structures, our strategy may be characterized by the use of palladium's 90 degree coordination angle because synthetic chemists have never employed this angle to construct their target structures.

VII-J-1 Made-to-Order Assembling of [2]Catenanes from Palladium(II)-Linked Rectangular Molecular Boxes

Makoto FUJITA, Masaru AOYAGI (Grad. Univ. Adv. Stud.), Fumiaki IBUKURO (Grad. Univ. Adv. Stud.), Katsuyuki OGURA (Chiba Univ.) and Kentaro YAMAGUCHI (Chiba Univ.)

[*J. Am. Chem. Soc.* **120**, 611 (1998)]

Linked-ring molecules or catenanes have long intrigued chemists because mechanically connected structures are expected to show unique properties which chemically connected molecules have never possessed. An ideal methodology for catenane synthesis should allow chemists to design and prepare a variety of catenanes in quantitative yields without synthetic difficulties. Here we show such an ideal catenane synthesis can be provided by metal-mediated supramolecular self-assembly. That is, designed molecular boxes composed of transition metals and organic ligands are quantitatively catenated if the boxes involve parallelly arranged aromatic sides with the interplane separation of ca 3.5 Å. Thus eight building blocks — four metals and four ligands — are found to self-assemble into [2]catenanes **1** and **2** consisting of two rectangular molecular boxes.



VII-J-2 Self-Assembled Molecular Ladders

Makoto FUJITA, Osamu SASAKI (Chiba Univ.), Kenya WATANABE (Chiba Univ.), Katsuyuki OGURA (Chiba Univ.) and Kentaro YAMAGUCHI (Chiba Univ.)

[*New. J. Chem.* 189 (1998)]

Coordination of a pyridine-based bridging ligand, 1,4-bis(4-pyridylmethyl)benzene, with cadmium nitrate afforded an infinite ladder complex, the unit structure of which involves a T-shaped assembly of three pyridine rings about a heptacoordinated Cd(II) atom. The ladder structure was found to expand its cavity volume by enclathrating *p*-dibromobenzene in the cavity. Nearly orthogonal interpenetration of infinite ladders was observed in the solid structure.

VII-J-3 Coordination Polymers Self-

Assembling from Cadmium(II) Ions and Flexible Pyridine-Based Bridging Ligands

Makoto FUJITA, Masaru AOYAGI (*Grad. Univ. Adv. Stud.*) and Katsuyuki OGURA (*Chiba Univ.*)

[*Bull. Chem. Soc. Jpn.* **71**, 1799 (1998)]

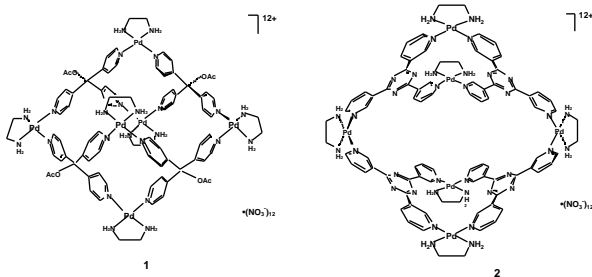
This paper describes coordination polymers assembling from cadmium nitrate and flexible bridging ligands, Py-X-Py (Py = 4-pyridyl, **1a**: X = CH₂, **1b**: X = C(=CH₂), **1c**: X = CH₂CH₂). Single X-ray analysis of these complexes showed that their infinite topologies are quite different from each other despite the structural similarity of ligands **1a-1c**. Upon treatment with Cd(NO₃)₂, **1a** gave a sheet structure of an infinite two-dimensional network with a stoichiometry of ML₂ (M and L denote metal and ligand, respectively). Ligand **1b** also afforded an infinite polymer possessing the same ML₂ composition. However the polymer structure is characterized by a one-dimensionally bounded macrocyclic frameworks where adjacent Cd ions are linked by two ligand molecules. Interestingly, ligand **1c** gave an infinite polymer of ML_{1.5} composition whose structure was shown to be a unique one-dimensional framework having macrocyclic frameworks (M₂L₂) linked by different L molecules.

VII-J-4 Nanometer-Sized Macrotricyclic Complexes Self-Assembled from Ten Small Component Molecules

Makoto FUJITA, Shu-Yan YU, Takahiro KUSUKAWA, Hidenori FUNAKI (*Chiba Univ.*), Katsuyuki OGURA (*Chiba Univ.*) and Kentaro YAMAGUCHI (*Chiba Univ.*)

[*Angew. Chem. Int. Ed. Engl.* **37**, 2082 (1998)]

Self-assembly of nanoscale, highly positive charged macrotricycles **1** and **2** with a general formula of [M₆L₄]¹²⁺ (where M = (en)Pd(II), L = tripyridyl ligands) is described. Both complexes have macrotricyclic structures with the dimension of ca. 3 nm × 2 nm × 2 nm which were unambiguously determined by X-ray crystallographic analysis. Having large hydrophobic cavities, they showed unique ability for molecular recognition of aromatic carboxylate ions. A proposed pathway leading to the [M₆L₄]¹²⁺ macrotricycles involves an intermediate macrocycle [M₂L₂]⁴⁺ which was isolated in a related system and structurally characterized by X-ray analysis.



VII-J-5 Encapsulation of Large, Neutral Molecules in a Self-Assembled Nanocage Incorporating Six Palladium(II) Ions

Takahiro KUSUKAWA and Makoto FUJITA

[*Angew. Chem.* **110**, 2192 (1998)]

The synthesis of hollow, nanometer-scale molecular "container compounds" makes possible the creation of localized chemical micro-environments with properties different from those of the bulk phases. Recently, a hollow, roughly spherical nanocage framework (**1**, ca 2 nm in diameter) was constructed by self-assembly from ten species, four organic ligands held together by six metal ions.[1] Herein reported is binding property of nanocage **1** with large guest molecules. It is shown that self-assembled cage **1** can hold as many as four adamantane molecules inside its nanosized cavity. Thus efficient formation of **1**·G₄ complex (G = adamantane) in a two-phase system was observed when D₂O solution of **1** was stirred with saturated hexane solution of adamantane at 60°C (Figure 1). Cage compound **1** also encapsulates as many as four molecules of o-carborane (8 Å in diameter). A large guest, 1,3,5-tri-tert-butylbenzene, once encapsulated through thermally-activated slippage, cannot escape from the cavity at room temperature since its dimension is slightly larger than that of the cavity entrance.

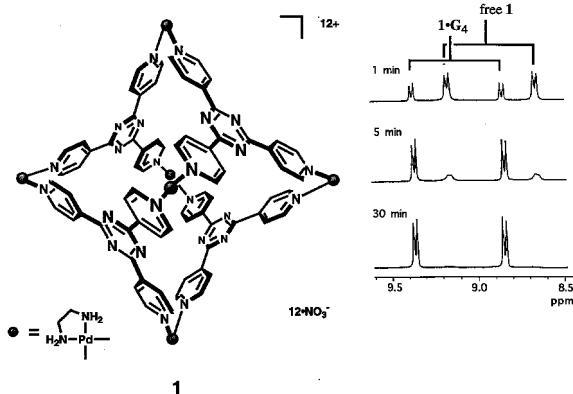


Figure 1. Time-dependent NMR observation of aq phase in the formation of **1**·G₄ complex through liquid-liquid extraction (aq phase: D₂O solution of **1**; org phase: saturated hexane solution of G.)

VII-J-6 A Thermally Switchable Molecular Lock. The Guest-Templated Synthesis of a Kinetically Stable Nano-Sized Cage

Fumiaki IBUKURO (*Grad. Univ. Adv. Stud.*), Takahiro KUSUKAWA and Makoto FUJITA

[*J. Am. Chem. Soc.* **120**, (1998)]

Metal-containing supramolecules are in general labile and not tolerant under acidic, basic, or nucleophilic conditions because they self-assemble as a result of thermodynamic equilibration. If the self-assembled structures can be converted to kinetically inert structures, then supramolecules in thermodynamic

equilibration can be trapped into kinetically stable forms. Such a conversion was achieved by exploiting the dual character of a Pt(II)-pyridine coordinate bond which is inert but temporally becomes labile by thermal stimuli. Thus, stable nano-sized cage complex **1** self-assembled under thermal stimuli and converted into an inert (stable) form by turning off the thermal stimuli. A large guest molecule showed remarkable template effect for the conversion. In addition, the complete switching of the binding property of cage **1** by pH control was achieved.

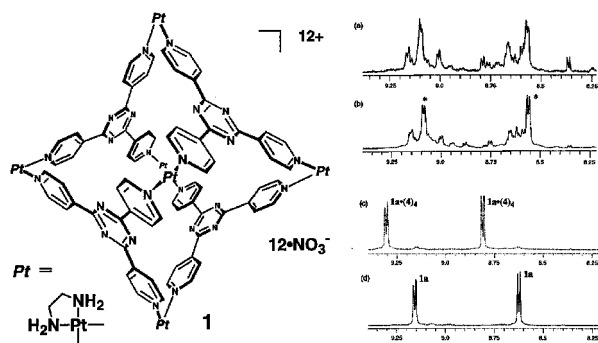


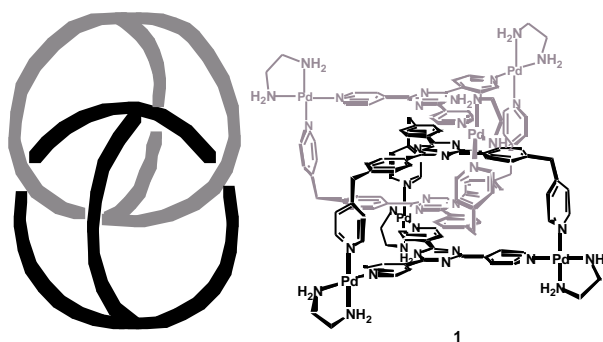
Figure 1. The ^1H NMR observation of the guest template synthesis of **1a** (500 MHz, D_2O , 25°C , TMS as an external standard). (a) A kinetically distributed oligomer mixture. (b) After 24 h at 100°C . Main peaks (*) assignable to **1a** appear at 9.08 and 8.56, which are slightly upfield shifted (by ca 0.05 ppm) from those of empty **1a** presumably due to some interactions with other oligomer components. (c) After 24 h at 100°C in the presence of guest **4** (4 equiv). Signals appearing at $\delta = 9.31$ and 8.81 are assigned to **1a**-(**4**)₄ and slightly downfield shifted from those of empty **1a**. (d) Empty cage **1a** obtained after the removal of guest **4** (acid form) by extraction with CHCl_3 .

VII-J-7 Spontaneous Assembling of Ten Small Components into a Three-Dimensionally Interlocked Compound Consisting of the Same Two Cage Frameworks

Makoto FUJITA, Norifumi FUJITA (*Grad. Univ. Adv. Stud.*), **Katsuyuki OGURA** (*Chiba Univ.*) and **Kentaro YAMAGUCHI** (*Chiba Univ.*)

Recent developments in noncovalent syntheses are partly thanks to the achievement of the efficient syntheses of catenanes by metal-templating as well as by self-assembly. While a catenane framework stems from the topological isomerism of two rings, no example has been reported to date for an interlocked molecule arising from the isomerism of two cages. Here, we show that such a three-dimensionally interlocked compound consisting of two cages, as schematically shown in Figure 1a, is easily prepared by metal-mediated self-assembly. The framework of each cage is self-assembled from five components, two different exo-tridentate ligands held together with three metal ions. The cage framework possesses an interplanar separation with a distance ideal to bind an aromatic ring. Thus, the two cage units efficiently bind each other through the formation of an efficient quadruple aromatic stack giving rise to a ten-component self-

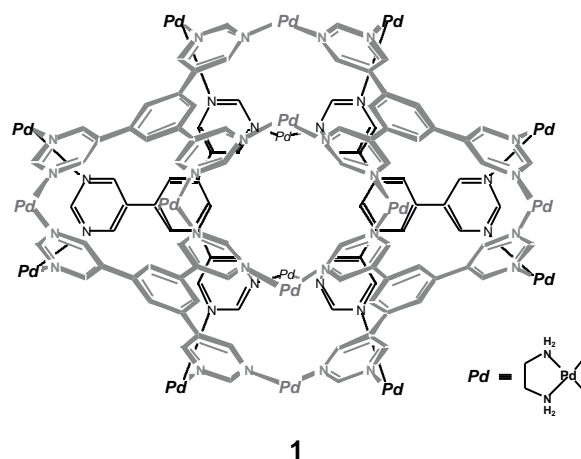
assembly into an unprecedented three-dimensionally interlocked molecule **1**.



VII-J-8 A Nonmeter-sized Hexahedral Coordination Capsule Assembled from Eighteen Metal Ions and Six Triangular Organic Ligands

Nobuhiro TAKEDA (*CREST, Science and Technology Corporation (JST) and IMS*), **Kentaro YAMAGUCHI** (*Chiba Univ.*) and **Makoto FUJITA**

Molecular capsules create isolated microspace inside their frameworks where molecules, once encapsulated, cannot interact with any outside species. In such isolated space, the properties of molecules can change and, for example, otherwise unstable molecules can be remarkably stabilized. Here we report the transition metal-induced assembly of a stable, nanometer sized coordination capsule **1** from twenty-four small components, eighteen metals and six triangular organic ligands. Capsule **1** is roughly hexahedral and made up of six edge-sharing triangles with two metal ions at each side. The triangular unit is composed of four coplanar aromatic rings. Thus, totally twenty-four aromatic rings surround the large cavity of capsule **1** making a closed shell structure with small pinhalls through which ordinary organic molecules can never come in nor escape.



VII-J-9 "Ship-in-a-Bottle" Formation of Stable Hydrophobic Dimers of cis-Azobenzene and -Stilbene Derivatives in a Self-Assembled Coordination Nanocage

Takahiro KUSUKAWA and Makoto FUJITA

Stabilization and activation of molecules in the cavity of cage-like molecules have been receiving increasing attention. A recent rapid progress in this field is partly owing to the development of facile preparation of cage compounds by non-covalent synthesis exploiting hydrogen and coordination bonds. Nano-sized coordination cage **1**, recently constructed by transition metal-mediated self-assembly, has been

shown to enclathrate large neutral guest molecules. Here we report the selective enclathration of "C-shaped" molecules such as cis-azobenzene and -stilbene derivatives by cage **1**. These guest molecules are enclathrated in the cavity through the "ship-in-a-bottle assembly" into a hydrophobically interacted dimer with a topology reminiscent of Rebek's hydrogen bonded "tennis ball" (eq 1). We also show that the hydrophobic dimers of azobenzene derivatives are considerably stabilized and do not undergo cis-trans isomerization.

VII-K Synthesis and Reactivity of Complexes Containing Peculiar Bonds between Transition Elements and Main Group Elements of Group 14

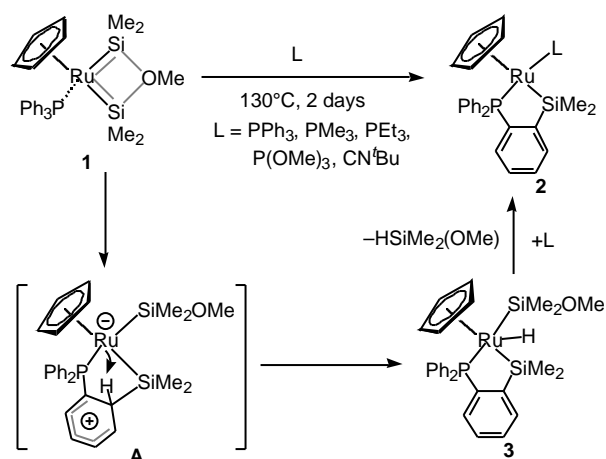
The bonds between transition elements and main group elements are attracting increasing attention in recent years. This is attributable not only to the great variety of the combination of elements but also to the peculiarity of their physical and chemical properties. We focused on transition metal complexes containing novel and peculiar bonds between transition elements and some main group elements of group 14, particularly multiple bonds to silicon and germanium. Some new silyl and silylene complexes and their germanium analogs were prepared and the reactivity of these complexes was examined to gain a better understanding on the unsaturated bond systems involving silicon and germanium atoms. In addition, the reactivity and properties of M-Si single bonds and the C-H bond activation by cationic metallocenes were investigated.

VII-K-1 Intramolecular Aromatic C-H Bond Activation by a Silylene Ligand in a Methoxy-Bridged Bis(silylene)-Ruthenium Complex

Hiroaki WADA (*Tohoku Univ.*), **Hiromi TOBITA** (*Tohoku Univ. and IMS*) and **Hiroshi OGINO** (*Tohoku Univ.*)

[*Organometallics* **16**, 3870 (1997)]

When a solution of Cp(Ph₃P)Ru{SiMe₂...O(Me)...SiMe₂} (**1**; Cp = ⁵-C₅H₅) and a two-electron-donating ligand L was heated at 130°C, a C-H bond of a phenyl group was activated by the Ru=Si double bond, and the complexes CpLRuSiMe₂(*o*-C₆H₄PPh₂) (**2a**, L = PPh₃; **2b**, L = PMe₃; **2c**, L = PEt₃; **2d**, L = P(OMe)₃; **2e**, L = ^tBuNC) were obtained. Heating **1** in the absence of a ligand at 130°C gave CpLRuSiMe₂(*o*-C₆H₄PPh₂)-(H)(SiMe₂OMe) (**3**). A possible mechanism for formation of **2** involves the electrophilic attack of a silylene ligand to the ortho carbon of a phenyl group in the PPh₃ ligand to give **A**. Subsequent proton migration to the Ru center gives **3**, and when a two-electron donor L exists, reductive elimination of HSiMe₂OMe and addition of L occur to afford **2**. This is the first example of C-H bond activation by a silylene complex.

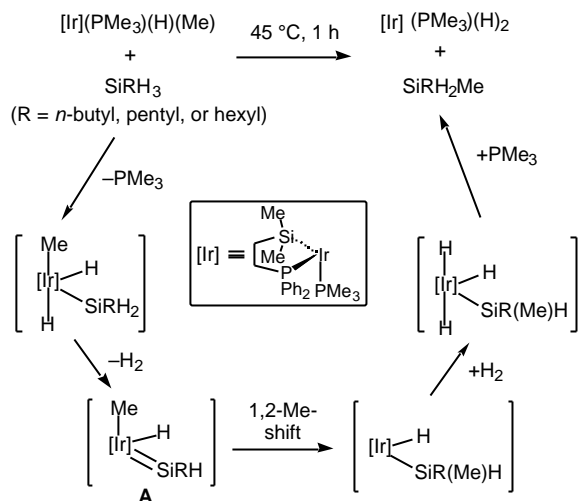


VII-K-2 Quantitative Transfer of a Methyl Group from a Methyl(hydrido)iridium Complex to SiRH₃ (R = *n*-butyl, pentyl or hexyl) to Give SiR(Me)H₂ and a Dihydridoiridium Complex

Masaaki OKAZAKI (*Tohoku Univ.*), **Hiromi TOBITA** (*Tohoku Univ. and IMS*) and **Hiroshi OGINO** (*Tohoku Univ.*)

[*J. Chem. Soc., Dalton Trans.* 3531 (1997)]

Thermal reaction of [Ir(Me)(H){²-Me₂Si(CH₂)₂-PPh₂}(PMe₃)₂] with SiRH₃ (R = *n*-butyl, pentyl, or hexyl) resulted in silicon-carbon bond formation to give SiR(Me)H₂ and [IrH₂{²-Me₂Si(CH₂)₂PPh₂}(PMe₃)₂]. Isolation of Si(*n*-C₆H₁₃)MeH₂ was achieved by preparative gas chromatography. A possible mechanism involving 1,2-methyl-shift in hydrido(methyl)(silylene) intermediate **A** was proposed.

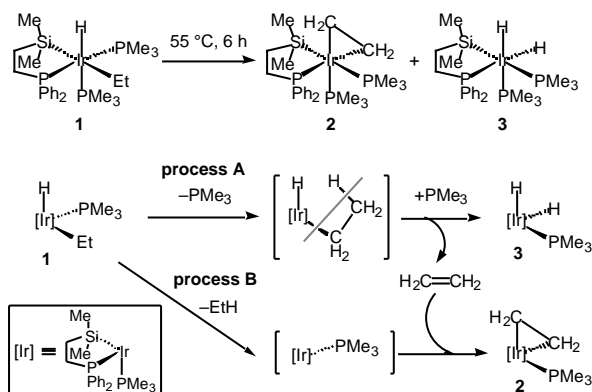


VII-K-3 Thermal Reaction of Ethyl(hydrido){(2-phosphinoethyl)silyl}iridium(III) Complex — Formation of a {(2-Phosphinoethyl)}(ethene)iridium(I) Complex —

Masaaki OKAZAKI (*Tohoku Univ.*), Hiromi TOBITA (*Tohoku Univ. and IMS*) and Hiroshi OGINO (*Tohoku Univ.*)

[*Chem. Lett.* 69 (1998)]

Thermolysis of $L_n\text{Ir}(\text{C}_2\text{H}_5)(\text{H})$ (**1**) [$L_n = \{^2\text{-Me}_2\text{-Si}(\text{CH}_2)_2\text{PPh}_2\}(\text{PMe}_3)_2$] led to the clean formation of a 1:1 mixture of ethene complex $L_n\text{Ir}(\text{C}_2\text{H}_4)$ (**2**) and dihydrido complex $L_n\text{Ir}(\text{H})_2$ (**3**). The geometry of these products were unequivocally determined by NMR spectroscopy. A possible mechanism involves a parallel occurrence of two processes; (**A**) reversible elimination of ethene and (**B**) irreversible reductive elimination of ethane. The ethene generated in process **A** is effectively trapped by the coordinatively unsaturated species formed in process **B**. The ethene complex **2** is proved to be an efficient precursor of an unsaturated silyliridium(I) species through dissociation of ethene.

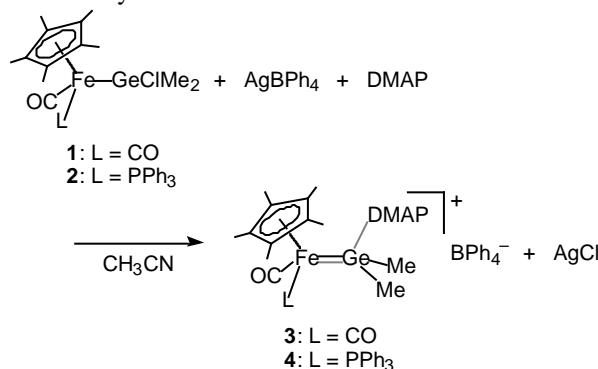


VII-K-4 Synthesis of Cationic Germyleneiron Complexes and X-Ray Structure of $[\text{Cp}^*(\text{CO})_2\text{Fe}=\text{GeMe}_2\text{-DMAP}]\text{BPh}_4\cdot\text{CH}_3\text{CN}$ ($\text{Cp}^* = \text{C}_5\text{Me}_5$, DMAP = 4-(Dimethylamino)pyridine)

Hiromi TOBITA (*Tohoku Univ. and IMS*), Kaoru ISHIYAMA (*Tohoku Univ.*), Yasuro KAWANO (*Tohoku Univ.*), Shinji INOMATA (*Tohoku Univ.*) and Hiroshi OGINO (*Tohoku Univ.*)

[*Organometallics* 17, 789 (1998)]

Chlorogermyl iron complexes $\text{Cp}^*(\text{CO})_2\text{FeGeMe}_2\text{-Cl}$ (**1**) and $\text{Cp}^*(\text{CO})(\text{PPh}_3)\text{FeGeMe}_2\text{-Cl}$ (**2**) undergo chloride abstraction by AgBPh_4 in the presence of 4-(dimethylamino)pyridine (DMAP) to afford cationic germylene complexes $[\text{Cp}^*(\text{CO})_2\text{Fe}=\text{GeMe}_2\text{-DMAP}]\text{BPh}_4$ (**3**) and $[\text{Cp}^*(\text{CO})(\text{PPh}_3)\text{Fe}=\text{GeMe}_2\text{-DMAP}]\text{BPh}_4$ (**4**), respectively. Structural determination by X-ray crystallography of **1** and **3**· CH_3CN revealed that both complexes have a gauche conformation with respect to the Fe-Ge bonds. The short Fe-Ge bond (2.329(3) Å) and very long Ge-N (DMAP) bond (1.989(8) Å) in **3**· CH_3CN demonstrate the unsaturated bond character of the former and the dative bond character of the latter. The complexes **3** and **4** in dichloromethane revert to the parent complexes **1** and **2**, respectively, via an electron transfer process from the counter anion, BPh_4^- , followed by chlorine abstraction from the solvent.



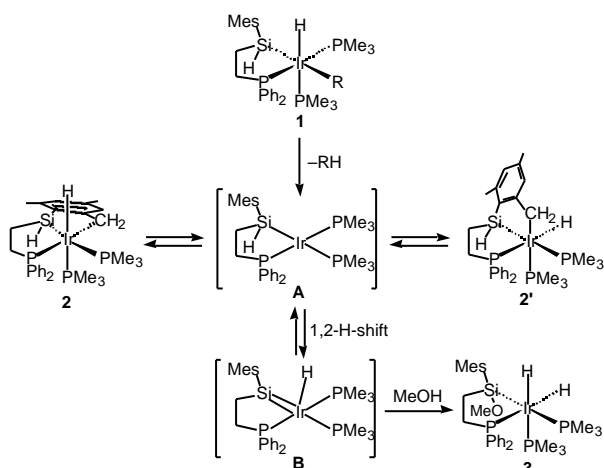
VII-K-5 Thermal Reactions of Alkyl(hydrido)-(hydrosilyl)iridium(III) Complexes: Generation of a Hydrido(silylene)iridium(I) Species via the Reductive Elimination of Alkane and 1,2-H-Shift from the Silicon Atom to the Ir(I) Metal Center

Masaaki OKAZAKI (*Tohoku Univ.*), Hiromi TOBITA (*Tohoku Univ. and IMS*), Yasuro KAWANO (*Tohoku Univ.*), Shinji INOMATA (*Tohoku Univ.*) and Hiroshi OGINO (*Tohoku Univ.*)

[*J. Organomet. Chem.* 553, 1 (1998)]

Heating of alkyl(hydrido)(hydrosilyl)iridium(III) complexes $L_n\text{Ir}(\text{R})(\text{H})$ (**1**) [$L_n = \{^2\text{-MesHSi}(\text{CH}_2)_2\text{-PPh}_2\}(\text{PMe}_3)_2$, R = Me, Et] led to the reductive elimination of alkane. Subsequently, the resulting hydrosilyliridium(I) intermediate $L_n\text{Ir}$ (**A**) activated the intramolecular carbon-hydrogen bond to give two geometrical isomers of $\text{Ir}(\text{H})(^3\text{-CH}_2\text{C}_6\text{H}_2(\text{CH}_3)_2\text{SiH}(\text{CH}_2)_2\text{PPh}_2)(\text{PMe}_3)_2$ (**2** and **2'**). In the presence of MeOH, **A** was quickly trapped with MeOH to give a methoxysilyliridium(III) complex $\text{Ir}(\text{H})_2\{^2\text{-Mes}(\text{MeO})\text{Si}(\text{CH}_2)_2\text{PPh}_2\}(\text{PMe}_3)_2$ (**3**). This reactivity of **A** with MeOH clearly supports the occurrence of a 1,2-H-shift from the silyl silicon atom to the iridium center to

generate a hydrido(silylene)iridium(I) species $\text{Ir}(\text{H})[\text{=SiMe}_2(\text{CH}_2)_2\text{PPh}_2](\text{PMe}_3)_2$ (**B**).

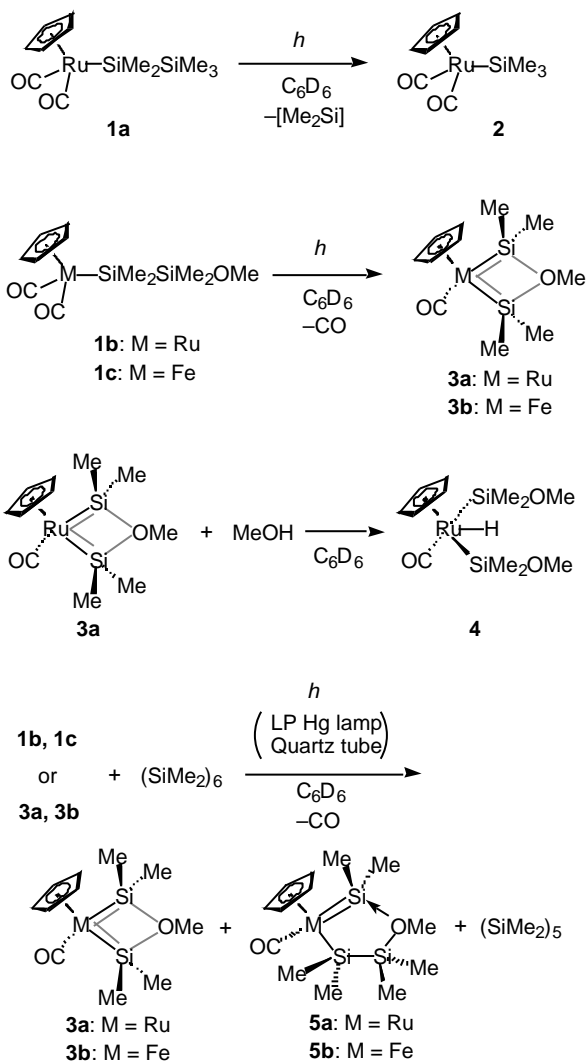


VII-K-6 Synthesis, Structure, and Reactivity of a Bis(silylene)(carbonyl)ruthenium Complex and a Novel Addition Reaction of Photochemically Generated Dimethylsilylene to Bis(silylene) Complexes $\text{Cp}(\text{OC})\text{M}\{\text{SiMe}_2\cdots\text{O}(\text{Me})\cdots\text{SiMe}_2\}$ ($\text{M} = \text{Ru}, \text{Fe}$)

Hiromi TOBITA (*Tohoku Univ. and IMS*), **Hitoe KURITA** (*Tohoku Univ.*) and **Hiroshi OGINO** (*Tohoku Univ.*)

[*Organometallics* **17**, 2844 (1998)]

Photolysis of $\text{CpRu}(\text{CO})_2\text{SiMe}_2\text{SiMe}_3$ (**1a**) with a low or medium pressure Hg lamp for a long time caused the loss of a SiMe_2 moiety to give $\text{CpRu}(\text{CO})_2\text{SiMe}_3$ (**2**) perhaps through the photochemical dissociation of a CO ligand. This mechanism was supported by the quantitative formation of bis(silylene)ruthenium complex $\text{Cp}(\text{OC})\text{Ru}\{\text{SiMe}_2\cdots\text{O}(\text{Me})\cdots\text{SiMe}_2\}$ (**3a**) by photolysis of (methoxydisilanyl)ruthenium complex $\text{CpRu}(\text{CO})_2\text{SiMe}_2\text{SiMe}_2\text{OMe}$ (**1b**). The X-ray crystal structure analysis of **3a** revealed that **3a** has an almost planar Ru-Si-O-Si four-membered chelate ring with short Ru-Si bonds (2.316(3) and 2.311(3) Å) and long Si \cdots O bonds (1.801(7) and 1.793(7) Å). **3a** reacts with MeOH instantaneously to give $\text{Cp}(\text{OC})\text{Ru}(\text{H})(\text{SiMe}_2\text{OMe})_2$ (**4**) quantitatively. Photolysis of $\text{CpM}(\text{CO})_2\text{SiMe}_2\text{SiMe}_2\text{OMe}$ (**1b**: $\text{M} = \text{Ru}$, **1c**: $\text{M} = \text{Fe}$) or $\text{Cp}(\text{OC})\text{M}\{\text{SiMe}_2\cdots\text{O}(\text{Me})\cdots\text{SiMe}_2\}$ (**3a**: $\text{M} = \text{Ru}$, **3b**: $\text{M} = \text{Fe}$) with a photochemical silylene precursor $(\text{SiMe}_2)_6$ by means of a low pressure Hg lamp afforded a mixture of **3a** or **3b**, disilanyl(silylene) complexes $\text{Cp}(\text{OC})\text{M}\{\text{SiMe}_2\text{O}(\text{Me})\text{SiMe}_2\text{SiMe}_2\}$ (**5a**: $\text{M} = \text{Ru}$, **5b**: $\text{M} = \text{Fe}$), and $(\text{SiMe}_2)_5$. Two possible mechanisms for the addition of dimethylsilylene to **3** to give **5** were proposed.



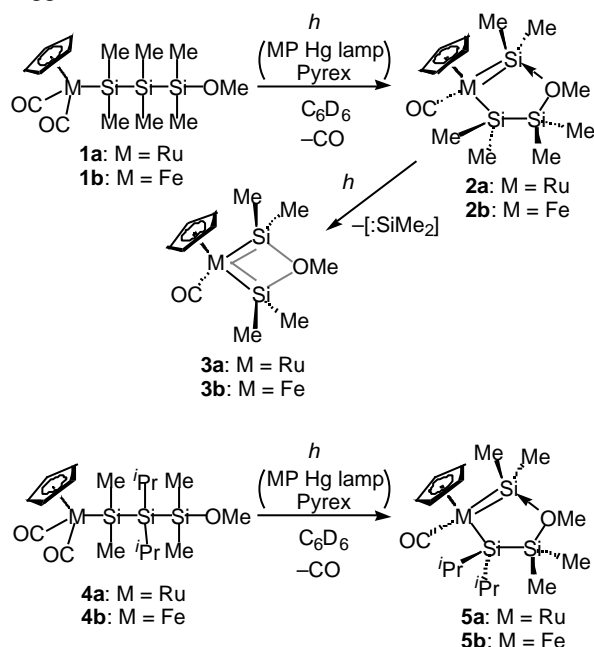
VII-K-7 Synthesis and Properties of Intramolecularly Base-Stabilized Disilanyl(silylene)ruthenium and -iron Complexes

Hiromi TOBITA (*Tohoku Univ. and IMS*), **Hitoe KURITA** (*Tohoku Univ.*) and **Hiroshi OGINO** (*Tohoku Univ.*)

[*Organometallics* **17**, 2850 (1998)]

Photolysis of 3-methoxytrisilanyl complex $\text{CpM}(\text{CO})_2\text{SiMe}_2\text{SiMe}_2\text{SiMe}_2\text{OMe}$ (**1a**: $\text{M} = \text{Ru}$, **1b**: $\text{M} = \text{Fe}$) afforded intramolecularly methoxy-stabilized disilanyl(silylene) complex $\text{Cp}(\text{OC})\text{M}\{\text{SiMe}_2\text{O}(\text{Me})\text{SiMe}_2\text{SiMe}_2\}$ (**2a**: $\text{M} = \text{Ru}$, **2b**: $\text{M} = \text{Fe}$) as a primary product. Prolonged irradiation of the solution resulted in the decay of **2a,b** with release of a dimethylsilylene moiety to give methoxy-bridged bis(silylene) complex $\text{Cp}(\text{OC})\text{M}\{\text{SiMe}_2\cdots\text{O}(\text{Me})\cdots\text{SiMe}_2\}$ (**3a**: $\text{M} = \text{Ru}$, **3b**: $\text{M} = \text{Fe}$). The X-ray crystal structure analysis of **2a** revealed that **2a** has a 5-membered chelate ring and the Ru-Si(silylene) bond (2.291(2) Å) is much shorter than the other Ru-Si bond (2.350(1) Å). It can be concluded from the bond lengths that the former possesses a partial double bond character while the latter is a normal Ru-Si single bond.

Photolysis of diisopropyl derivatives $\text{CpM}(\text{CO})_2\text{SiMe}_2\text{-Si}^i\text{Pr}_2\text{SiMe}_2\text{OMe}$ (**4a**: $\text{M} = \text{Ru}$, **4b**: $\text{M} = \text{Fe}$) gave $\text{Cp}(\text{OC})\text{M}\{\text{=SiMe}_2\text{ O}(\text{Me})\text{SiMe}_2\text{Si}^i\text{Pr}_2\}$ (**5a**: $\text{M} = \text{Ru}$, **5b**: $\text{M} = \text{Fe}$) exclusively, in which the positions of substituents on silicon atoms in **5a** and **5b** were determined by ^{29}Si - ^1H COLOC and NOESY NMR spectra. Mechanism involving 1,2-migration of the methoxydisilanyl group to the metal center was suggested.

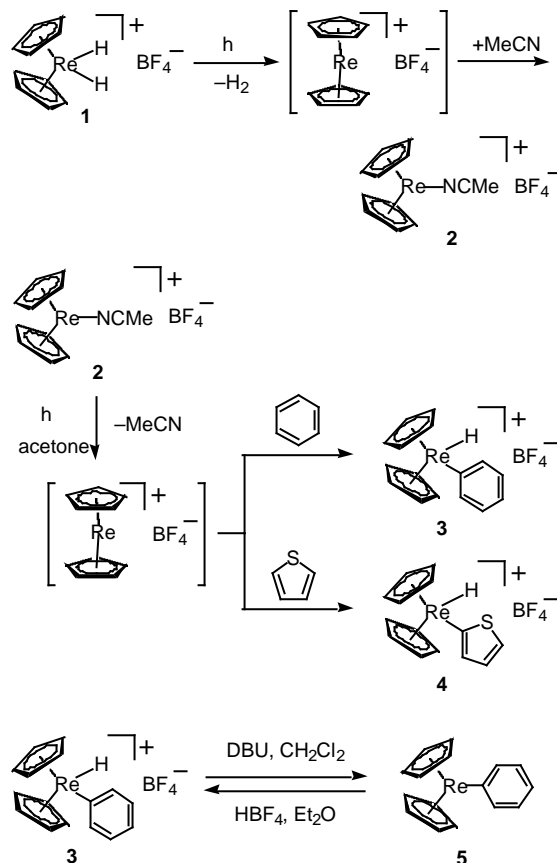


VII-K-8 Thermal and Photochemical Reactions of a Cationic Rhenocene-Acetonitrile Adduct: The First C-H Bond Activation by Rhenocene Cation

Hiromi TOBITA (Tohoku Univ. and IMS), Kiyonari HASHIDZUME (Tohoku Univ.), Kouji ENDO (Tohoku Univ.) and Hiroshi OGINO (Tohoku Univ.)

[*Organometallics* **17**, 3405 (1998)]

Photolysis of $[\text{Cp}_2\text{Re}(\text{H})_2](\text{BF}_4)$ (**1**) in MeCN afforded $[\text{Cp}_2\text{Re}(\text{NCMe})](\text{BF}_4)$ (**2**) as moderately air and moisture stable red crystals in 93% isolated yield. Complex **2** did not react with benzene or thiophene thermally at room temperature, but under UV irradiation **2** reacted with an excess of benzene and thiophene to give the C-H bond activation products $[\text{Cp}_2\text{Re}(\text{H})\text{Ph}](\text{BF}_4)$ (**3**) and $[\text{Cp}_2\text{Re}(\text{H})(2\text{-C}_4\text{H}_3\text{S})](\text{BF}_4)$ (**4**) in 88% and 80% yields, respectively. Small kinetic isotope effect ($k_{\text{H}}/k_{\text{D}} = 1.09$) was measured for the formation reaction of **3**. The cationic complex **3** was readily deprotonated by DBU to give phenylrhenocene Cp_2RePh (**5**) in 70% yield. This reaction is reversible and the protonation of **5** with HBF_4 regenerated **3** in 85% yield.



VII-K-9 Novel Reaction of Silyl Carbonyl Complexes with Hydride-Transfer Reagents: Reduction of a Carbonyl Ligand and Coupling with a Silyl Group

Rie SHIOZAWA (Tohoku Univ.), Hiromi TOBITA (Tohoku Univ. and IMS) and Hiroshi OGINO (Tohoku Univ.)

[*Organometallics* **17**, 3497 (1998)]

Treatment of $(^5\text{-C}_5\text{R}'_5)\text{Fe}(\text{CO})_2\text{SiR}_3$ ($\text{R}' = \text{H}, \text{CH}_3$; $\text{R} = \text{H}, \text{alkyl}, \text{aryl}$) with LiAlH_4 in ether or THF gave CH_3SiR_3 as a major product in moderate to high yield together with HSiR_3 . Labeling experiments using LiAlD_4 and ^{13}C proved that the carbonyl ligand was reduced with LiAlH_4 and coupled with the silyl group to give the methylsilane.

